

**DESIGN A NEUROFEEDBACK SYSTEM WITH
INCORPORATED REAL TIME EOG ARTIFACT
REMOVAL**

HO JUN LEONG

UNIVERSITI TUNKU ABDUL RAHMAN

**DESIGN A NEUROFEEDBACK SYSTEM WITH INCORPORATED REAL
TIME EOG ARTIFACT REMOVAL**

HO JUN LEONG

**A project report submitted in partial fulfilment of the
requirements for the award of Bachelor of Engineering
(Honours) Electronic Engineering**

**Faculty of Engineering and Green Technology
Universiti Tunku Abdul Rahman**

April 2022

DECLARATION

I hereby declare that this project report is based on my original work except for citations and quotations which have been duly acknowledged. I also declare that it has not been previously and concurrently submitted for any other degree or award at UTAR or other institutions.

Signature : 

Name : Ho Jun Leong

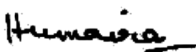
ID No. : 18AGB01556

Date : 24 April 2022

APPROVAL FOR SUBMISSION

I certify that this project report entitled **“DESIGN A NEUROFEEDBACK SYSTEM WITH INCORPORATED REAL TIME EOG ARTIFACT REMOVAL”** was prepared by **HO JUN LEONG** has met the required standard for submission in partial fulfillment of the requirements for the award of Bachelor of Engineering (Hons) Electronic Engineering at Universiti Tunku Abdul Rahman.

Approved by,

Signature : 

Supervisor : Prof. Ts. Dr. Humaira Nisar

Date : 04.05.2022

The copyright of this report belongs to the author under the terms of the copyright Act 1987 as qualified by Intellectual Property Policy of Universiti Tunku Abdul Rahman. Due acknowledgement shall always be made of the use of any material contained in, or derived from, this report.

© 2022, Ho Jun Leong. All rights reserved.

Specially dedicated to
my beloved father, mother, and brother

ACKNOWLEDGEMENTS

I would like to thank everyone who had contributed to the successful completion of this project. I had a chance to research neuroscience and improved my knowledge in this field. I would like to express my gratitude to my project supervisor, Professor Dr. Humaira Nisar for allowing me to develop a BCI system for neurofeedback application and for invaluable advice, guidance as well as enormous patience throughout the development of the project.

In addition, I would also like to express my gratitude to my loving parent and friends who had helped and given me encouragement throughout the whole development of this project. I will not be able to complete this project without their help. Once again, I sincerely thank everyone for the help, guidance, and encouragement provided throughout the development of this project.

DESIGN A NEUROFEEDBACK SYSTEM WITH INCORPORATED REAL TIME EOG ARTIFACT REMOVAL

ABSTRACT

Electroencephalography (EEG) is the electrophysiological, non-invasive method that can record the activities of the brain. It can use the electrodes that are attached to the scalp to detect the brain signal (Arefa Cassoobhoy, MD, MPH, 2020). Neurofeedback training (NFT) which is a training method that uses the Brain Computer Interface (BCI) to improve the cognition performance of the subjects. Artifacts in EEG are the signals not associated with the brain activities and these signals may affect the NFT process. So, it is important to remove artifacts from EEG signals. In our project, we will design a neurofeedback system to perform the real-time EOG artifact removal. The artifact removal is one of the pre-processing steps in the BCI system that removes the unwanted noise from the raw EEG signals. The method used for artifact removal is ICA-REG. the BCI system is designed by using the EMOTIV Insight headset to collect EEG signals, OpenViBE for processing the EEG signal, and the Unity3D application for the interface of the BCI system. We will use this BCI system to perform NFT for 6 subjects in 6 sessions and analyze the EEG data recorded from the subjects.

TABLE OF CONTENTS

DECLARATION	ii
APPROVAL FOR SUBMISSION	iii
ACKNOWLEDGEMENTS	vi
ABSTRACT	vii
TABLE OF CONTENTS	viii
LIST OF TABLES	x
LIST OF FIGURES	xii
LIST OF ABBREVIATIONS	xv

CHAPTER

1	INTRODUCTION	1
	1.1 Background	1
	1.2 Problem Statements	7
	1.3 Aims and Objectives	7
2	LITERATURE REVIEW	8
	2.1. The main parts of the human brain	8
	2.2. The Lobes of the human brain	9
	2.3. Brain Signals	10
	2.4. EEG Headset	12
	2.5. Types of Artifacts	16
	2.6. Blind Source Separation (BSS)	18
	2.7. Independence Components Analysis (ICA)	19

	2.8.	Regression Method	23
	2.9.	BCI important elements for neurofeedback application	26
	2.10.	Summary	32
3		METHODOLOGY	34
	3.1.	Overview	34
	3.2.	EEG Headset and computer requirement	35
	3.3.	EMOTIV PRO	38
	3.4.	OpenViBE	41
	3.5.	MATLAB for OpenViBE scripting	47
	3.6.	Unity3D	47
	3.7.	Neurofeedback training	51
	3.8.	MATLAB for data analysis	53
	3.9.	Budget	54
4		RESULT AND DISCUSSION	55
	4.1.	Artifact removal by using ICA-REG	55
	4.1.1.	The working of ICA-REG	56
	4.1.2.	Advantages of using ICA-REG	58
	4.1.3.	Result of the ICA-REG	59
	4.2.	Data Analysis from the NFT training	61
	4.2.1.	Correlation	62
	4.2.2.	Root Mean Square Error	65
	4.2.3.	Alpha band power	68
5		RECOMMENDATIONS AND CONCLUSIONS	74
	5.1	Future work and Recommendations	74
	5.2	Conclusion	75
		REFERENCE	76
		APPENDICES	87
		APPENDIX A: MATLAB SCRIPT FOR OPENVIBE	87
		APPENDIX B: MATLAB SCRIPT FOR DATA ANALYSIS	90

LIST OF TABLES

TABLE	TITLE	PAGE
Table 2.1:	The naming rule in International 10/20 System.	14
Table 2.2:	The comparison between standard EEG and high density EEG.	15
Table 2.3:	The details of the methods of interface that were used in the enhanced mu suppression experiment (Hyunmi & JeongHun, 2018).	27
Table 2.4:	The amount of improvement for each indicator of the virtual group and real group (Dong-Kyun, Min-Ho, John & Seong-Whan, 2019).	30
Table 3.1:	Technical Specifications for EMOTIV Insight Headset (EMOTIV, n.d.).	36
Table 3.2:	Technical Specifications for the Desktop Computer.	37
Table 3.3:	The setting of the LSL in the EMOTIV PRO.	40
Table 3.4:	The budget of this project.	54
Table 4.1:	The correlation of the EEG recorded signal from Subject 1 to Subject 3.	63
Table 4.2:	The correlation of the EEG recorded signal from Subject 4 to Subject 6.	64
Table 4.3:	The RMSE of the EEG recorded signal from Subject 1 to Subject 3.	66
Table 4.4:	The RMSE of the EEG recorded signal from Subject 4 to Subject 6.	67
Table 4.5:	The Alpha power of the EEG recorded signal from Subject 1 and Subject 2.	69
Table 4.6:	The Alpha power of the EEG recorded signal from Subject 3 and Subject 4.	70
Table 4.7:	The Alpha power of the EEG recorded signal from Subject 5 and Subject 6.	71

Table 4.8: The Alpha power of all subjects in session before training and after training.

LIST OF FIGURES

FIGURE	TITLE	PAGE
	Figure 1.1: Hans Berger (David, 2014).	2
	Figure 1.2: The early EEG graph recorded by Hans Berger (Wikiwand, n.d.).	2
	Figure 1.3: The brain map (Living Well Dallas, 2019).	3
	Figure 1.4: The Brain Computer Interface.	3
	Figure 1.5: The signal source in different types of brain signals (NeuroTech, n.d.).	4
	Figure 2.1: The main parts of the human brain (Johns Hopkins Medicine, n.d.).	8
	Figure 2.2: The human brain anatomy (Johns Hopkins Medicine, n.d.).	9
	Figure 2.3: Two neurons communicate with the chemical and electrical signals (Anping Huang, 2018).	10
	Figure 2.4: The 5 main types of brainwaves (Muse, 2018).	11
	Figure 2.5: The International 10/20 System for the EEG (Sleep Tech Study, 2013).	12
	Figure 2.6: The skull landmark (Sleep Tech Study, 2013).	13
	Figure 2.7: The skull landmark with bone (ERS, 2016).	13
	Figure 2.8: The high density EEG (Lebonheur, n.d.).	15
	Figure 2.9: The recorded EEG signal, pure EEG signal, and different types of artifacts (Xiao Jiang, Gui-Bin Bian, and Zean Tian, 2019).	16
	Figure 2.10: Cocktail party problem.	18
	Figure 2.11: The original signals in the ICA test.	20
	Figure 2.12: The mixed signals in the ICA test.	21
	Figure 2.13: The independence components signals in the ICA test.	21

Figure 2.14: The model of the regression method (Shailaja Kotte and J R K Kumar Dabbakuti, 2020).	23
Figure 2.15: The adaptive filter (Adaptive Filters, 2015).	23
Figure 2.16: The flickering video in frames (Hyunmi & JeongHun, 2018).	26
Figure 2.17: The four methods for the enhanced mu suppression experiment (Hyunmi & JeongHun, 2018).	26
Figure 2.18: The mu rhythm suppression result of QEEG for all four methods.	27
<i>Figure 2.19: The mu rhythm suppression main effect that shows in radial form</i>	27
Figure 2.20: The virtual and real environment neurofeedback training (Dong-Kyun, Min-Ho, John & Seong-Whan, 2019).	28
Figure 2.21: The Stroop test and digital span test (Dong-Kyun, Min-Ho, John & Seong-Whan, 2019).	28
Figure 2.22: The QEEG result of alpha band power (Dong-Kyun, Min-Ho, John & Seong-Whan, 2019).	29
Figure 2.23: The 2D game stimulus content (2D-GSC) (Yasir, Syed, Syed, Muhammad, Syed, 2019).	30
Figure 2.24: The 3D game stimulus content (3D-GSC) (Yasir, Syed, Syed, Muhammad, Syed, 2019).	31
Figure 2.25: The mean value of prefrontal alpha asymmetry for G1–NFT and G2–NFT (Yasir, Syed, Syed, Muhammad, Syed, 2019).	31
Figure 3.1: The basic flow of the BCI system.	34
Figure 3.2: EMOTIV Insight Headset.	35
Figure 3.3: The electrode placement of the EMOTIV Insight (EMOTIV, n.d.).	36
Figure 3.4: The solution for the headset electrode.	37
Figure 3.5: The wireless Bluetooth USB.	37
Figure 3.6: The contact quality of each electrode.	38
Figure 3.7: The signal quality of each electrode.	39
Figure 3.8: The EEG signal in the time-domain.	39
Figure 3.9: The setting of the LSL export in EMOTIV PRO.	40
Figure 3.10: The message window for the OpenViBE Acquisition Server.	41

Figure 3.11: The setting in OpenViBE Acquisition Server.	41
Figure 3.12: The setting of the driver properties.	42
Figure 3.13: The interface of the OpenViBE Designer.	43
Figure 3.14: The message window for the OpenViBE Designer.	44
Figure 3.15: The boxes and the connection in the OpenViBE Designer for the NFT training.	44
Figure 3.16: The setting for the channel selector.	44
Figure 3.17: The setting of the MATLAB scripting.	45
Figure 3.18: The setting for the temporal filter in Alpha band frequency.	45
Figure 3.19: The setting for the channel selector that chooses AF3 and AF4 channels.	46
Figure 3.20: The setting of the LSL export.	46
Figure 3.21: The window of creating a new project.	48
Figure 3.22: The interface of the Unity3D.	48
Figure 3.23: The example scene for the LSL data receiver.	49
Figure 3.24: The scene for the LSL data for the project.	49
Figure 3.25: The build setting of the Unity3D.	50
Figure 3.26: The logo of unity when entering the program.	50
Figure 3. 27: The interface of the LSL data receiver program.	50
Figure 3.28: The way of wearing the headset.	51
Figure 3.29: The whole process of NFT training.	51
Figure 3.30: The neurofeedback training.	52
Figure 3.31: The neurofeedback training.	52
Figure 4.1: The whole process of ICA-REG.	56
Figure 4.2: The kurtosis compares with the normal distribution (Misha Sv, 2021).	56
Figure 4.3: The raw EEG and the EOG free EEG signal.	60
Figure 4.4: The raw EEG and the EOG free EEG signal 2.	60
Figure 4.5: The raw EEG and the EOG free EEG signal 3.	61
Figure 4.6: The graph of the raw signal Alpha power in NFT training.	72
Figure 4.7: The graph of the clean signal Alpha power in NFT training.	72

LIST OF ABBREVIATIONS

ADHD	Attention Deficit Hyperactivity Disorder
BCI	Brain Computer Interface
BMI	Brain Machine Interface
BSS	Blind Source Separation
ECoG	Electrocorticography
ECG	Electrocardiogram
EEG	Electroencephalography
EMG	Electromyography
EOG	Electrooculography
IC	Independent Component
ICA	Independent Components Analysis
NFB	Neurofeedback
NFT	Neurofeedback Training
QEEG	Quantitative Electroencephalography
REG	Regression
RMSE	Root Mean Square Error

CHAPTER 1

INTRODUCTION

1.1 Background

The brain is the most complex organ in our body. It not only can control all the body movements but also can memorize, think, imagine and represent emotions. It's like the control center of the whole body. Even though there is a lot of functionality, we can't understand fully the brain. The scientist from MIT, Matt Wilson says that the human brain is extremely unique and inscrutable but we can still gain enough of those basic principles to copy and emulate the functions (Lindsay Patterson, 2009). So, the discovery and research of the brain are very popular topics nowadays.

If we need to know or understand brain activities, we need to research the signal that is produced by the brain. Electroencephalography (EEG) is the electrophysiological method that can record the activities of the brain. It can use the electrodes that are attached to the scalp to detect the brain signal (Arefa Cassoobhoy, MD, MPH, 2020). The brain is active all the time, so the EEG can record the brain activities anytime even the person is sleeping (Nitin Sreedhar, 2020).



Figure 1.1: Hans Berger (David, 2014).

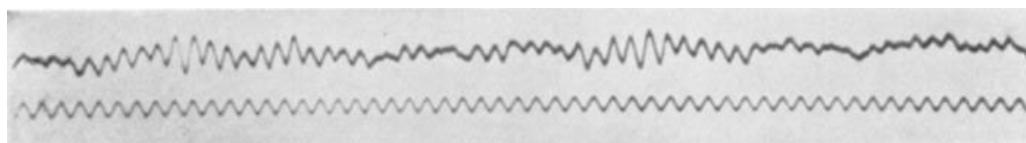


Figure 1.2: The early EEG graph recorded by Hans Berger (Wikiwand, n.d.).

The history of EEG can refer back to the last century. In 1924, a German psychiatrist Hans Berger has recorded the first EEG during neurosurgery performed by neurosurgeon Nikolai Guleke (1878–1958). Later, he developed a brain signals recording method. This method is connecting the electrode to the scalp is the same as present-day and he was the first person to record a non-invasive electrical activity of the human brain. In 1929, he published his first paper on EEG, “Über das Elektrenkephalogramm des Menschen,” using the terms alpha and beta waves (Rümeysa, Saliha, Fatma, 2020).

There are many applications for human EEG research. The first one is neuro-marketing. The economists use EEG research to detect the consumers’ brain activities when they decide or purchase the products and their mental state when exploring the physical or virtual stores. Next, the EEG is also used in psychology and neuroscience. Most of the time, psychological studies utilize EEG to study the brain processes underlying attention, learning, and memory. Furthermore, it also can be used in clinical and psychiatric studies. The EEG data from patients’ brains can help doctors accurately determine the symptoms and give the treatment to the patients. Lastly, it can use in the Brain Computer Interface (BCI). It can use to build a tool without any physical movement. For example, the BCI can use a controller for a device such as game control, robot control,

or even vehicles (iMotions, 2015). It also can use as a communication device with the computer without any external hardware.

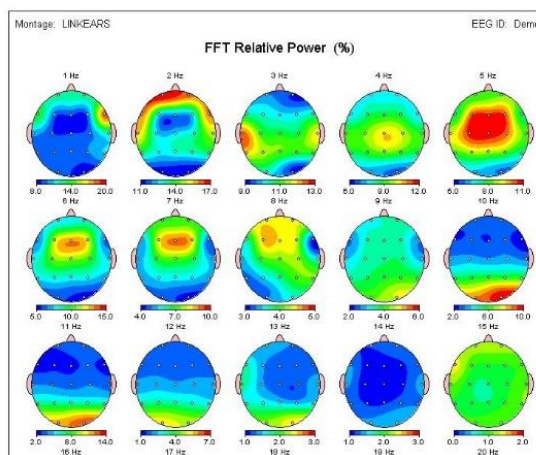


Figure 1.3: The brain map (Living Well Dallas, 2019).

The EEG has an involved technique called Quantitative Electroencephalography (QEEG), which is the analysis of digitized EEG. It is a technique that processed the recorded EEG activities from the multi-channel recording using a computer. This multi-channel EEG data is processed with various algorithms, such as the Fourier series (QEEG support, n.d.). The QEEG is commonly converted into a colorful brain map as shown in *Figure 1.3*. This method can help scientists more understand EEG and the function of the brain.

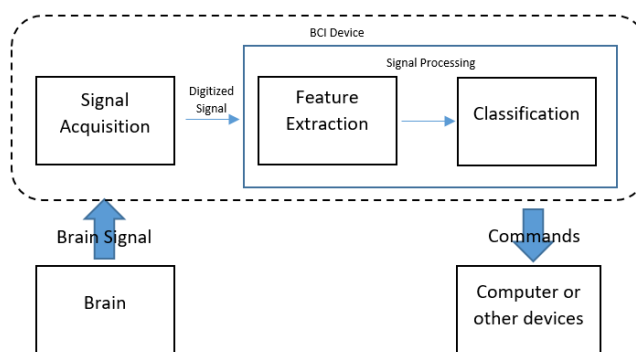


Figure 1.4: The Brain Computer Interface.

The Brain Computer Interface (BCI) is one of the applications of the EEG. The Brain Computer Interface also known as Brain Machine Interface (BMI), is a device that can communicate between the human brain and the computer. Its working principle is a closed-loop or feedback system that which the device has received the brain signal from the human brain by using the EEG and it would give the response to the human. After the human saw the response of the device and makes the change to the device by using the brain signal (Joseph, 2010).

There are few applications for BCI such as medical treatment, robot control, research of the brain, and communication with the computer. Medical treatment is one of the applications for BCI. It can be used for brain training for Attention Deficit Hyperactivity Disorder (ADHD), Depressive, anxiety disorders, and for the patients that need to recover from the brain injury. It also can help patients that blind or paralyzed. Next, the BCI can be used for robot control. The robot hand or leg with the BCI system can help disabled people to solve inconvenient problems. Furthermore, the BCI can be used for research purposes. It can record the real-time brain signal and present it through the display screen. Scientists can use the real-time brain signal to gain more information from the human brain. Lastly, the BCI can communicate with the computer. The computer needed to record the user's brain signals and it will follow certain brain signals to show something or do specific tasks for the user.

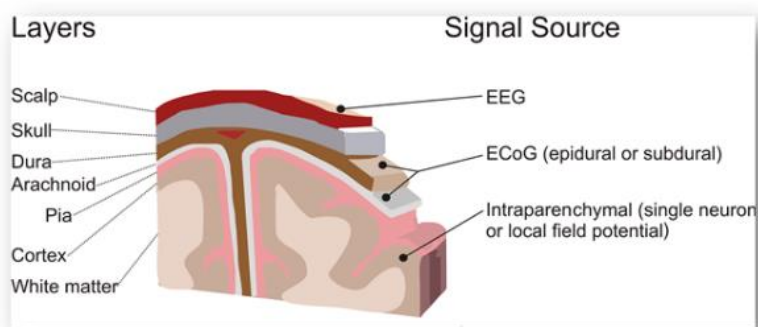


Figure 1.5: The signal source in different types of brain signals (NeuroTech, n.d.).

The BCI system can be categorized into three main types by the method of the detection of brain signals, one is invasive, one is semi-invasive and another is non-invasive. The invasive BCI signal is called the Intraparenchymal signal and its sensor is implanted directly into the brain during neurosurgery. It has the best quality of brain signal compared to another two methods but it has the risk of forming scar tissue to affect the sensor. This method is direct implanted, it has a high risk and cost of the surgery, so it is used in the patient for recovery of the blind and paralyzed (NeuroTech, n.d.).

Next, the depth of the electrodes in a semi-invasive BCI system is implanted between invasive and non-invasive BCI. Its method is called Electrocorticography (ECoG) in which the electrodes were implanted on the surface of the brain to measure electrical activity from the cerebral cortex. This method has more advantages such as noise resistance, higher amplitude, and lower clinical compared to invasive BCI. Due to ECoG being placed on the surface of the brain, to transmit the brain signal to the sensors, it doesn't need to go through the scrap which means it is not impacted by the signal caused by the muscles (EMG, Electromyography) and the eyes movements (EOG, Electrooculography). It also has a high amplitude signal due to less noise. Furthermore, it has less risk in the clinical compared to the invasive BCI. The electrodes don't need to penetrate the cortex, so it is safer than invasive BCI (NeuroTech, n.d.).

The most common BCI is the non-invasive BCI. The method of this BCI is using the EEG and the electrodes are placed on the scalp. It is used the less cost, hardware portability, and less time preparation but the signal amplitude is the weakest and its effectiveness is the lowest due to the noise from other parts of the body signal or movements. It is not suitable for extremely high accurate purposes (NeuroTech, n.d.).

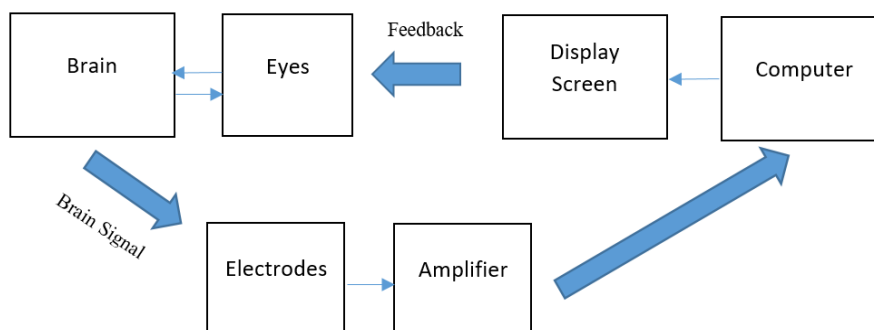


Figure 1.6: Neurofeedback system.

Although the BCI system can be used for the communication between the computer and the human brain, the human brain also needs to be trained before using BCI to increase its effectiveness. There is a brain training method called Neurofeedback (NFB). It is a form of biofeedback that provides real-time feedback on brain activity to encourage good brain function via operant training (Wikipedia, 2021). It means that we use a device to detect and show the brain activity and let the user know the data of the brain activity. After that, the user uses this real-time data to train the brain to reach a certain target. For example, there is an application that is used for focus training. The device was detected and recorded from a user's brain and it shows a beautiful picture to the user. The user needs concentration to maintain the color of the picture, if not reach the target it will start losing color and become black and white (Center for Brain, n.d.). The above *Figure 1.6* shows the basic neurofeedback system.

1.2 Problem Statements

In this project, we will design a non-invasive BCI. Due to the non-invasive nature of our project, EEG signals are highly prone to noise. Noisy or artifactual EEG signals may lead to improper NFT. For BCI applications, it is important to have good EEG electrodes contact quality with the scalp to ensure the amplitude and effectiveness of the brain signal. Generally, BCI applications are quite expensive. Thus, we will build a low-cost BCI for this project. Furthermore, the BCI used for NFT is working in real-time to observe and record the EEG data. Online artifact removal can be very resource expensive. So, we will find a suitable method for the artifact removal system for real-time application. Lastly, we need to collect sufficient data from the subjects to analyze the effect of real-time artifact removal on NFT.

1.3 Aims and Objectives

1. Acquisition of real-time EEG data and application of pre-processing methods such as signal decomposition and real-time artifact removal.
2. Designing a BCI system using real-time raw, and artifact removed EEG data for NFT.
3. Designing a user interface for NFT sessions displaying real-time alpha power to improve cognition and alertness.
4. Comparison of the effect of using raw EEG data and online artifact cleaned EEG data for NFT sessions.

CHAPTER 2

LITERATURE REVIEW

2.1. The main parts of the human brain

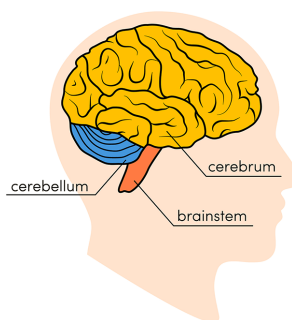


Figure 2.1: The main parts of the human brain (Johns Hopkins Medicine, n.d.).

The human brain is a complex organ that controls every activity in our body. It can divide into the cerebrum, cerebellum, and brain stem. The cerebrum is the largest part of the brain and it includes gray matter which is the cerebral cortex and white cortex. Its functions are to coordinate movement, regulate body temperature, enable senses, speech, judgment, memorization, thinking and reasoning, problem-solving, emotions, and learning. Next, the cerebellum also known as the little brain is a fist-sized portion of the brain located at the back of the head, below the temporal and occipital lobes, and above the brainstem. Its function is to coordinate voluntary muscle movements and maintain posture, balance, and equilibrium (Johns Hopkins Medicine, n.d.). Lastly, the brain stem

is one of the main parts of the human brain. It consists midbrain, pons, and medulla. Its main functions are to control automatic and involuntary activities like breathing, swallowing, blood pressure, and heart rate (BioNinja, n.d.).

2.2. The Lobes of the human brain

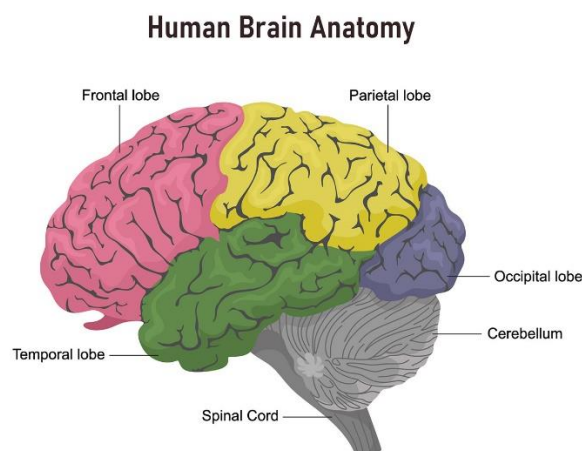


Figure 2.2: The human brain anatomy (Johns Hopkins Medicine, n.d.).

The cerebrum, there can divide into four sections which are the frontal, temporal, parietal, and occipital lobes as shown in **Figure 2.2**. The frontal lobe is the largest lobe and it's located at the front of our head. It involved critical thinking, problem-solving, decision making, and personality characteristic. It also contains Broca's area, which is associated with speech ability. Next, the temporal lobe is located at the side of the brain and it's integral to auditory perception, receptive components of language, visual memory, factual memory, and emotion (JueBin Huang, 2020). Furthermore, the parietal lobe is located at the top of the brain and it involves stimuli for recognition and generating visual-spatial relationships, and integrating these perceptions with other sensations to create awareness of the trajectories of moving objects (JueBin Huang, 2020). Lastly, the occipital lobe is located at the back of the brain and it mainly involved the vision (Johns Hopkins Medicine, n.d.) (BioNinja, n.d.).

2.3. Brain Signals

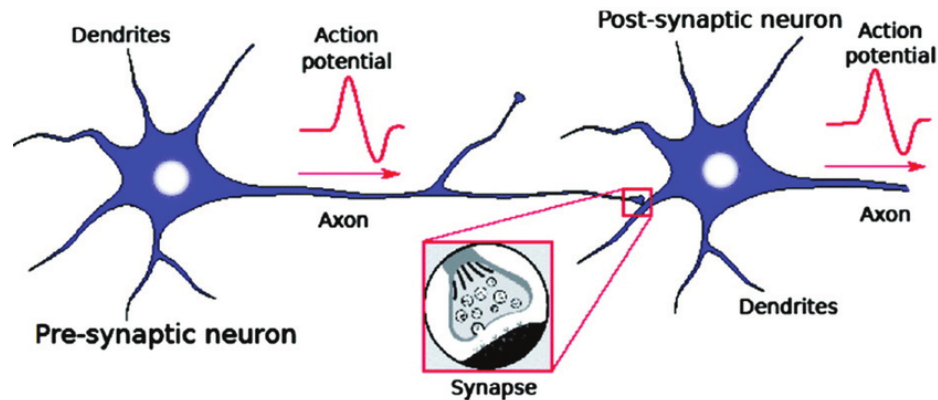


Figure 2.3: Two neurons communicate with the chemical and electrical signals (Anping Huang, 2018).

An average human brain has consisted of about 86 billion nerve cells or called neurons inside. These neurons communicate with each other using chemical and electrical signals (Georgia Chronaki, n.d.). The chemical and electrical signals are also called the action potential. When the action potential needs to transfer from the pre-synaptic neuron to the post-synaptic neuron, the signal needs to pass through the end of the pre-synaptic neuron called the synapse. The postsynaptic potential is the potential that makes the postsynaptic neuron more likely to fire an action potential (Wikipedia, n.d.). A single postsynaptic potential is very small, so there is a huge number of postsynaptic potentials being simultaneous and in the same direction are needed to total up to generate brain signals that can measure by EEG (Timo & Rudige, 2009).



Figure 2.4: The 5 main types of brainwaves (Muse, 2018).

The brain signals can divide into 5 main types of brainwaves by their frequency such as Alpha, Beta, Gamma, Delta, and Theta. Often the low-frequency brainwave has high amplitude and the high-frequency brainwave has low amplitude. The Delta wave is the slowest brainwave whose frequency range is within 0.1 to 4 Hz but it has the highest amplitude of these 5 brainwaves. It happens in deep and dreamless sleep and some abnormal processes. When the Delta wave increases, it will decrease our awareness of the physical world. Next, the brainwave that is slightly faster than the Delta wave is called the Theta wave. Its frequency range is between 4 to 8 Hz. It is strong when the person is in internal focus, prayer, meditation, daydreaming and spiritual awareness. It reflects the state between sleep and wakefulness and it also relates to the subconscious mind (Muse, 2018) (Neuro Health, n.d.).

Furthermore, the Alpha wave is the first discovered brainwave in which the frequencies range is between 8 to 12 Hz (Muse, 2018). It is very easy to detect when the eyes are closed and the mind is relaxed and its peak will always fall around 9 to 10 Hz. It happens when the person is physically and mentally relaxed which means it can be found before falling asleep or doing yoga. It is very important when you are learning and focusing on something (Neuro Health, n.d.). One of the studies shows that the Alpha wave is manipulating people's attention. In the attention experiment, If the Alpha wave of the

brain was suppressed, the people's visual cortex would have more response to the flashed light disturbed (Science Daily, 2019). So, the Alpha wave has played an important role in the attention.

Moreover, there is another brainwave called the Beta wave. It is faster than the three brainwaves mentioned in front but slower than the Gamma wave. Its frequency range is from 13 to 30 Hz. It can be easily detected when the person is active thinking like active conversation, making a decision, problem-solving, focusing on a task, and learning a new concept. It also can be measured if the person is in an alert state too (Muse, 2018). Lastly, the final brainwave is the Gamma wave. It is the fastest and the smallest amplitude brainwave among these five brainwaves. Its frequency is over 30 Hz. It can measure when the person is simultaneously processing information from different parts of the brain. It has been observed to be much stronger and commonly detected in very long-term meditators including Buddhist monks (Muse, 2018) (Neuro Health, n.d.).

2.4. EEG Headset

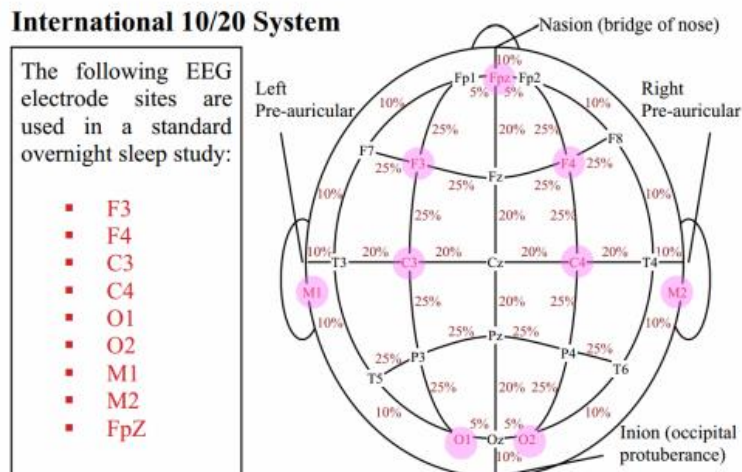


Figure 2.5: The International 10/20 System for the EEG (Sleep Tech Study, 2013).

The EEG can be divided into two types by the density of the electrodes. There are standard EEG and high-density EEG or called it hdEEG. The standard EEG is using the international 10/20 system for the placement of the electrodes. It is an internationally recognized method that allows EEG electrode placement to be standardized (ERS, 2016). The “10” and “20” mean that the distance of the electrodes that place needed to have 10% or 20% of the total distance front to back or left to right of the skull (Storti, 2013). It is needed to ensure inter-electrode spacing is equal and electrode placement is proportional to skull size and shape. So, before using the EEG headset, the researcher needed to measure the skull size of the subjects. According to the design and number of electrodes of the headset, there is also have 10/10 system and a 10/5 system (Robert, n.d.).

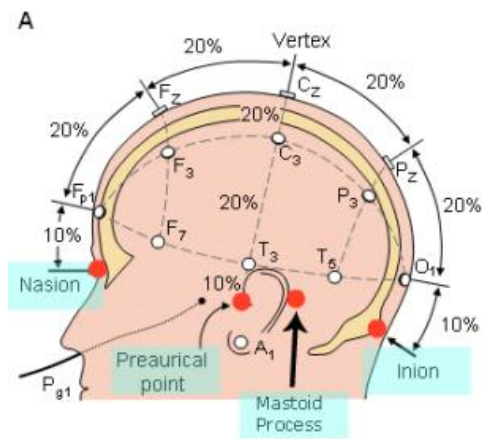


Figure 2.6: The skull landmark (Sleep Tech Study, 2013).

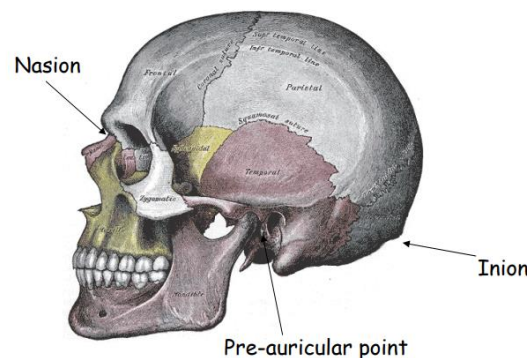


Figure 2.7: The skull landmark with bone (ERS, 2016).

There are four important skull landmarks such as nasion, inion, pre-auricular point, and mastoid. The starting point and the ending point for the front to back skull landmarks are the nasion and inion. The nasion is the bridge of the nose of the lowest point between nose and forehead. The inion is a bony ridge at the base of the back of the skull. Next, the pre-auricular point is the point that indentations just above the cartilage that covers the external ear openings. The last important skull landmark is on the bony area located just behind the ear where is also the M1 and M2 electrodes placed (Sleep Tech Study, 2013).

Table 2.1: The naming rule in International 10/20 System.

Electrodes Symbol and Number	Meaning
F	Frontal
T	Temporal
P	Parietal
O	Occipital
M	Mastoid
C	Central
Fp	Frontal pole
Even numbers	Right side
Odd numbers	Left side
z	Midline
A	Anterior

The electrodes placement has its naming rule. **Table 2.1** shows the naming rule for the placement of the electrodes. The F, T, P, O are mean for the Frontal, Temporal, Parietal and Occipital lobe. Next, the M and C are mean for the Mastoid and the Central point. The Fp is the point that is on the top of the nasion. Furthermore, the even number is mean the electrode points are all on the right side and the odd number is on the left side. Lastly, the z is the mean for the electrodes placed on the middle line. If two alphabets are named like “FC”, then the placement of the electrodes is between two specific areas. For example, “FC” is placed between the Frontal and Central (Trans Cranial Technologies, 2012). There is also another alphabet “A” which means Anterior also will use in the 10/20 system. For

example, the contour between the frontal pole (Fp) and the frontal (F) electrodes is called “AF” (Robert, n.d). The graph of the placement of the electrodes is shown in *Figure 2.6*.



Figure 2.8: The high density EEG (Lebonheur, n.d.).

There is another type of EEG called high-density EEG which it is using about 128 or 256 electrodes. It will have higher localization accuracy than the standard EEG but it needs to spend a lot of time to set up. Even with the experienced technician, the 128 electrodes EEG needed to spend 90 to 100 minutes to set up all the electrodes (Catherine, 2014). It is often used in high accuracy or clinical research such as diagnosis or evaluation of epilepsy (Lebonheur, n.d.).

Table 2.2: The comparison between standard EEG and high density EEG.

	Standard EEG	High Density EEG
Electrodes numbers	Less than 64 electrodes	128 or 256 electrodes
Set up time required	Less time	More time
Localization Accuracy	Low	High
Electrodes Density	Low	High
Application	Common brain research, BCI, clinical therapy, and Neurofeedback	High localization accuracy or clinical research like diagnosis or evaluation of epilepsy

2.5. Types of Artifacts

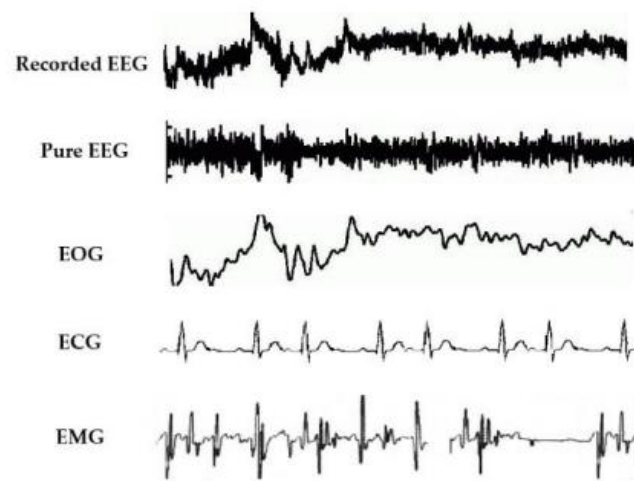


Figure 2.9: The recorded EEG signal, pure EEG signal, and different types of artifacts (Xiao Jiang, Gui-Bin Bian, and Zean Tian, 2019).

In the EEG signals recording, the unwanted signals will contaminate the EEG signals. These all unwanted signals are called artifacts. It will be directly affected the accuracy of the EEG signal, so it was needed to remove it in the pre-processing of the EEG data. There are a few types of the artifacts such as ocular artifact, muscle artifact, cardiac artifact, and technical artifacts (Bit Brain, 2020).

The ocular artifact comes from the human eyes which generate electrical dipoles. Eye movements and blinks cause the dipole to fluctuate, resulting in an electrical signal known as Electrooculography (EOG). It will cause a rapid, high-amplitude shift in the EEG signals in the frontal electrodes, which is particularly apparent in those adjacent to the eyes. Lateral eye motions influence the frontal regions of the EEG signals as well but have a greater impact as one gets closer to the temples. In general, the artefact amplitude is nearly proportional to the angle of vision (Bit Brain, 2020) (M. Agustina Garcés Correa and Eric Laciár Leber, 2014).

Next, the muscle artifact is the electrical activity that produces by the muscles. This electrical activity can be called Electromyography (EMG). It can be generated when the subjects are talking, swallowing, sucking, and chewing. It can be observed a high frequency signal that overlaps the EEG signal. Its amplitude will correlate to the EEG signal with the strength of the muscle contraction (Bit Brain, 2020).

Furthermore, the cardiac artifact is the electrical activity that comes from the heart pulsing. This signal is the scientific name known as Electrocardiogram (ECG). There is a rhythmic pattern, corresponding with the heartbeats that overlap the EEG signal. Although the amplitude of the ECG on the scalp is minimal, depending on the positioning of the electrode or the participant's body shape, we may notice a rhythmic distortion in the EEG data (Bit Brain, 2020).

Lastly, there are also have technical or non-physiological artifacts that affected the purity of the EEG signals. These types of artifacts include electrode pop, power line interference, and body movement. The electrode pop will happen if the electrode failed to contact the scalp or the electrode contact quality is bad. The effect from the electrode pop will make the observed EEG signal abrupt change and the amplitude is high. It is commonly localized in a single channel. The power line interference is the artifact that 50 or 60 Hz frequency interference which comes from wires, light fluorescents, and other equipment that are captured by the electrodes (M. Agustina Garc é s Correa and Eric Laciár Leber, 2014). This type of noise will continuously be overlapping the EEG signal. Another technical artifact is the body movement of the subject. Body movements like head movement, arm movement, or leg movement will affect the contact quality of the electrode with the scalp and corrupt the EEG signal (Bit Brain, 2020).

2.6. Blind Source Separation (BSS)

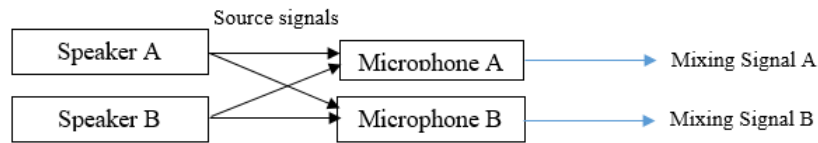


Figure 2.10: Cocktail party problem.

Blind Source Separation also known as Blind Signal Separation is a technique of image or signal processing to separate the mixing signals without knowing the source signals or mixing process. It doesn't need any extra reference to do the processing. The application for the BSS is used to solve the cocktail party problem. Let's assume a scenario for the cocktail party problem. Two speakers are using two microphones to speak and both are quite close to each other as shown in *Figure 2.10*. When they speak together at the same time, the two output voice signals will be mixed up from the two speakers. Both contaminated signals need to be processed to get the separate signals (Sanjeev, 2015).

The BSS is a good technique that processes the unknown mixing process of the mixing signal or the source signals. The equation can be shown in *Equation 2.1*. BSS technique inverts the mixing matrix to the unmixing matrix \mathbf{A}^{-1} to get the source signals as shown in *Equation 2.2*. If the mixing parameters inside the matrix \mathbf{A} are all knowledge and the mixing was truly linear, then it will be very easy to invert the mixing matrix \mathbf{A} . Unfortunately, the parameters in matrix \mathbf{S} and matrix \mathbf{A} were unknown which makes the BSS become complicated (Shadab, 2002). There is an algorithm called Independence Component Analysis (ICA) that can solve the problem. It will be introduced in *Section 2.7*.

$$\mathbf{X} = \mathbf{AS} \quad (2.1)$$

Where,

\mathbf{X} = observed signals

A = mixing matrix

S = source of the signals

$$\mathbf{X} = \begin{bmatrix} x_1(t) \\ x_2(t) \\ \vdots \\ x_n(t) \end{bmatrix}; \mathbf{S} = \begin{bmatrix} s_1(t) \\ s_2(t) \\ \vdots \\ s_n(t) \end{bmatrix}; \mathbf{A} = \begin{bmatrix} h_{11} & h_{12} & \cdots & h_{1m} \\ h_{21} & h_{22} & \cdots & h_{2m} \\ \vdots & \vdots & \cdots & \vdots \\ h_{n1} & h_{n2} & \cdots & h_{mn} \end{bmatrix}_{m=n}$$

$$\mathbf{S} = \mathbf{A}^{-1}\mathbf{X} \quad (2.2)$$

2.7. Independence Components Analysis (ICA)

Independence Component Analysis is an algorithm that can perform Blind Source Separation. It makes assumption on the parameters of the mixing square matrix A as shown in *Equation 2.2*. After estimating the matrix A , it needs to inverse become A^{-1} or named as matrix W and obtains the independence component as shown in *Equation 2.3*.

$$\mathbf{S} = \mathbf{A}^{-1}\mathbf{X} = \mathbf{W}\mathbf{X} \quad (2.3)$$

Where,

W = unmixing matrix

It needs to make a few assumptions before performing the ICA in the signal processing. The below is shows the assumptions for the ICA (Shadab Mozaffar & David W. Petr, 2002):

1. The statistical independence between each of the source s_n from the sources vector of S . The statistical independence means that the probability density function formula should follow *Equation 2.4* (Shadab Mozaffar & David W. Petr, 2002).

$$f(s_1, s_2, s_3, \dots, s_m) = f_1(s_1)f_2(s_2)f_3(s_3) \dots f(s_m) \quad (2.4)$$

2. The mixing matrix must be square and full rank. The rank is the number of the linear independence columns or rows. Thus, full rank means the number of the linear independence columns or rows is the largest possible for a matrix of the same dimension (Stat Trek, n.d.).
3. The number of the observed signals must be greater than or equal to the number of the independent signals. If can't be fulfilled means the observed signals don't have enough information for separation from the independent components (Shadab Mozaffar & David W. Petr, 2002).
4. The source signals must not be more than one signal that has a Gaussian signal (Shadab Mozaffar & David W. Petr, 2002).

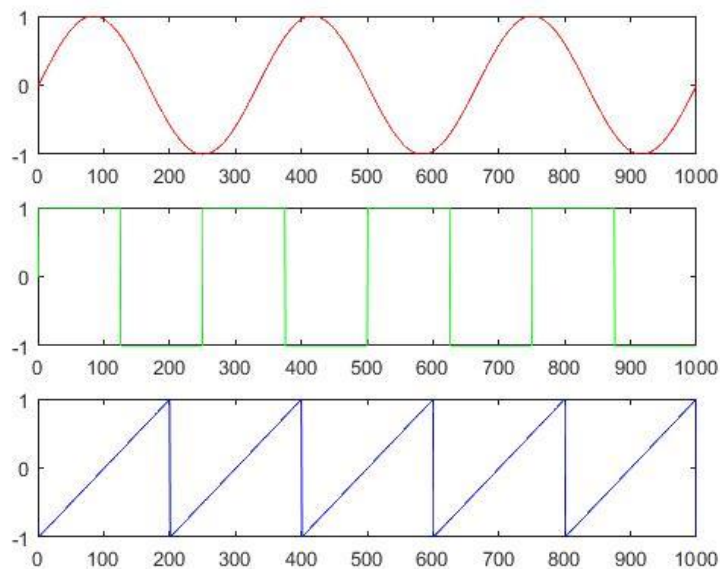


Figure 2.11: The original signals in the ICA test.

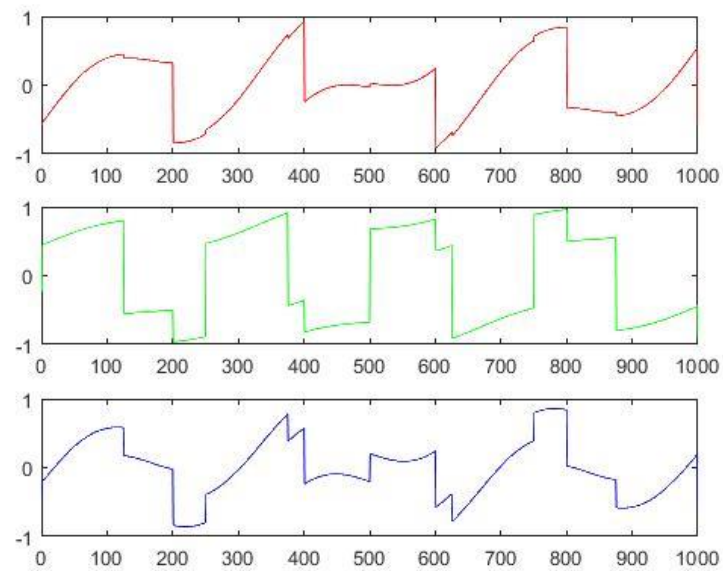


Figure 2.12: The mixed signals in the ICA test.

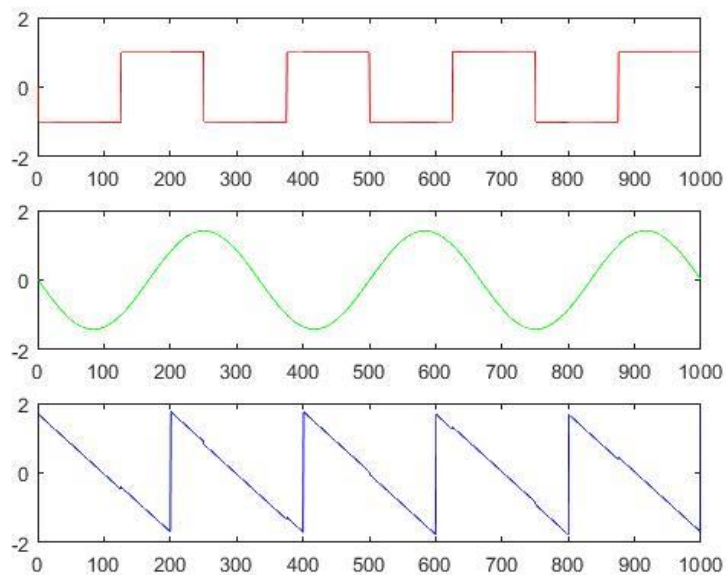


Figure 2.13: The independence components signals in the ICA test.

There are also have ambiguities in the ICA algorithm. The first ambiguity is ICA can't determine the variance or the energies of the independence components. In the ICA model, A and S are unknown, so it will assume the unit variance of the source signal component as 1: $E\{s_i^2\} = 1$. However, it may change the sign of the components when

the magnitude is -1. Fortunately, it can be solved by multiplying by -1. Thus, this ambiguity is insignificant in most of the applications. Next, the second ambiguity is the ICA can't determine the order of the independence components. The reason is that *Equation 2.1*, A and S are unknown at the starting point. So, the model can freely change the order of the term and call any independent components as the first one. The permutation matrix and its inverse matrix can insert inside *Equation 2.2* and form it as shown in *Equation 2.5*. The AP^{-1} is the new mixing matrix and the PS is the original independence signals with different orders (Hyvarinen & Oja, 2000).

$$\mathbf{X} = (\mathbf{AP}^{-1})(\mathbf{PS}) \quad (2.5)$$

2.8. Regression Method

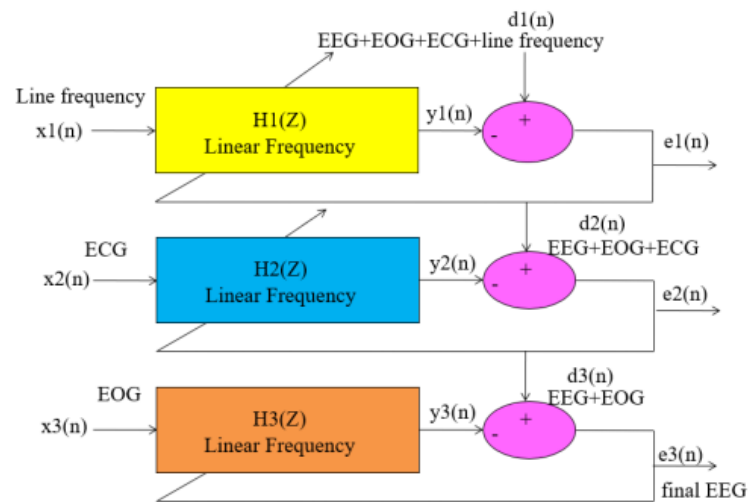


Figure 2.14: The model of the regression method (Shailaja Kotte and J R K Kumar Dabbakuti, 2020).

The regression method is a method that uses the amplitude relation of reference to estimate the artifact and remove it by following the reference signals. Therefore, this method needs to have external reference signals such as EOG, EMG, ECG, and power lines to separate the artifacts from the EEG signals (ShailajaKotte and J R K Kumar Dabbakuti, 2020). **Figure 2.14** shows the model of the regression method with three stages. Every stage consists of different types of artifacts reference signals. It will reduce each type of artifact after processing one stage.

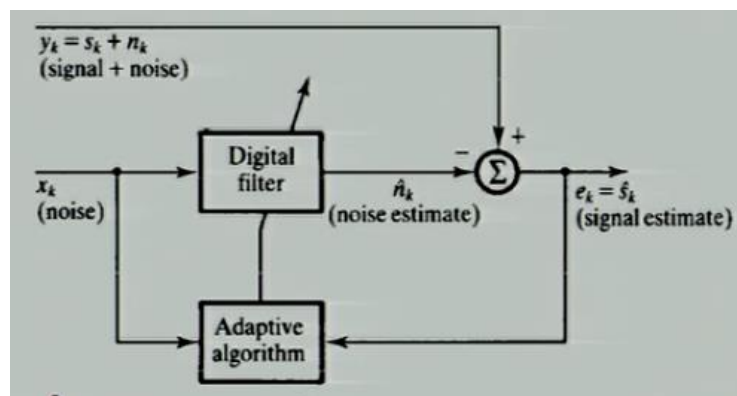


Figure 2.15: The adaptive filter (Adaptive Filters, 2015).

The regression method is using a few adaptive filters to perform. The adaptive filter is a filter that can remove the reference signal from the observed signal. There are two components that group the adaptive filter which is the digital filter and the adaptive algorithm as **Figure 2.15** shown. It needs to estimate the desired signal \hat{s}_k and produce the optimum noise \hat{n}_k by reference noise n_k to cancel the artifact to get the clean signal s_k from the contaminated signal y_k as shown in **Equation 2.6 and Equation 2.7**. Next, **Equation 2.8** is come from the squaring and mean of **Equation 2.9**. Due to the noise n_k and clean signal s_k are uncorrelated, the last term can be cancelled out and form the equation as shown in **Equation 2.10**. $E(\hat{s}_k^2)$ is represents the estimated signal power, $E(s_k^2)$ is represents the signal power and $E((n_k - \hat{n}_k)^2)$ represents the remnant noise power. If we need to get the maximum signal-to-noise ratio, the total output of the canceller will need to minimize (Adaptive Filters, 2015).

Contaminated signal:

$$y_k = s_k + n_k \quad (2.6)$$

Where,

y_k = contaminated signal

s_k = desired signal

n_k = reference noise

Estimate of the desired signal:

$$\hat{s}_k = y_k - \hat{n}_k = s_k + n_k - \hat{n}_k \quad (2.7)$$

Where,

\hat{n}_k = optimum noise

Squaring:

$$\widehat{s}_k^2 = s_k^2 + (n_k - \widehat{n}_k)^2 + 2s_k(n_k - \widehat{n}_k) \quad (2.8)$$

Mean:

$$E(\widehat{s}_k^2) = E(s_k^2) + E((n_k - \widehat{n}_k)^2) + 2E(s_k(n_k - \widehat{n}_k)) \quad (2.9)$$

$$E(\widehat{s}_k^2) = E(s_k^2) + E((n_k - \widehat{n}_k)^2) \quad (2.10)$$

2.9. BCI important elements for neurofeedback application

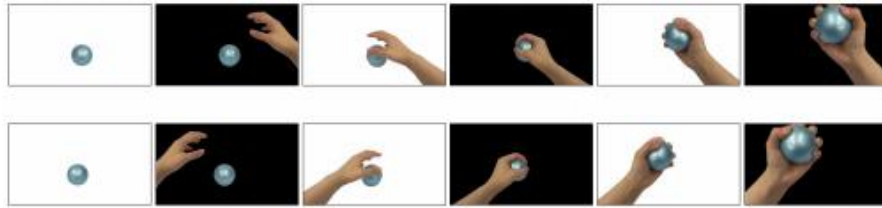


Figure 2.16: The flickering video in frames (Hyunmi & JeongHun, 2018).

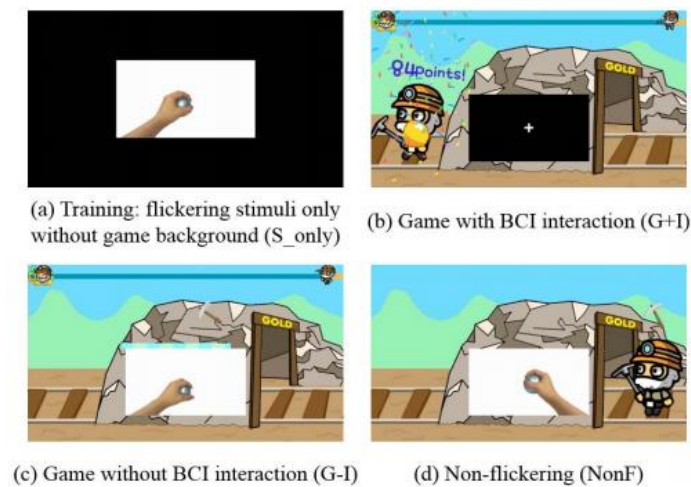


Figure 2.17: The four methods for the enhanced mu suppression experiment (Hyunmi & JeongHun, 2018).

The neurofeedback for BCI can be used as training to improve brain performance. Three elements are very important to improve the effectiveness of the BCI neurofeedback such as interactive, virtual environment stimulus, and 3-D stimulus. The first important element is the interaction of the BCI system. In one study, they have used different methods of interface to observe the result of attenuation mu band which this band frequency within 8 to 13 Hz. The experiment is used to measure using different methods of interface to enhance the mu suppression. The participants just need to stay focused on the screen to observe the result. There have used four methods in this experiment as flickering action video showing without game background (S_only), action observation game with BCI interactive (G + I), action observation game display without interactive

(G – I), and non-flickering stimuli with only game background (NonF). **Figure 2.16** shows the flickering video in frames. **Table 2.3** and **Figure 2.17** show all these four methods in the experiment (Hyunmi & JeongHun, 2018).

Table 2.3: The details of the methods of interface that were used in the enhanced mu suppression experiment (Hyunmi & JeongHun, 2018).

	S_only	G + I	G – I	NonF
Video Background	Flickering	Flickering	Flickering	Non-Flickering
Game Background	No	Yes	Yes	Yes
Game Observation	No	Yes	Yes	No
Measured attentiveness	No	Yes	No	No

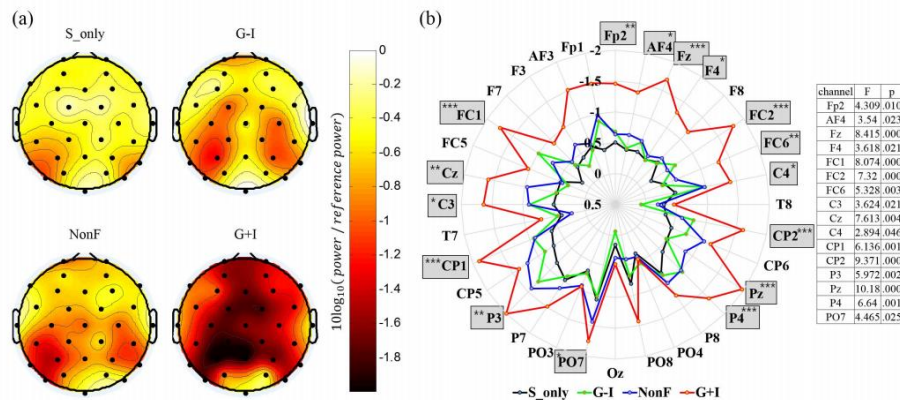


Figure 2.18: The mu rhythm suppression result of QEEG for all four methods.

Figure 2.19: The mu rhythm suppression main effect that shows in radial form (Hyunmi & JeongHun, 2018).

Figure 2.18 and *Figure 2.19* shows the rhythm suppression results of QEEG and radial form for every electrode. The method that uses the action observation game with BCI interactive has the most significant mu rhythm suppression compared to the other three methods. It means it has the most effective method among these methods. At the same time, the method that only uses the flickering action video showing without a game background has the least effective method. The result also shows that if the game loses the data feedback, the effectiveness of the neurofeedback system will have greatly reduced. The neurofeedback BCI system that hasn't any data interactive will have the same effect as the non-flickering stimuli with the only game background. So, the data feedback is the important thing in the neurofeedback BCI system to improve its effectiveness. (Hyunmi & JeongHun, 2018).



Figure 2.20: The virtual and real environment neurofeedback training (Dong-Kyun, Min-Ho, John & Seong-Whan, 2019).

	Stroop test			Digit span test	
Condition	Congruent	Incongruent	Control	Forward	Backward
Stimulus	<small>D=RED F=GREEN J=BLUE K=BLACK</small> 	<small>D=RED F=GREEN J=BLUE K=BLACK</small> 	<small>D=RED F=GREEN J=BLUE K=BLACK</small> 		
Response	Red	Green	Blue	29561	15348

Figure 2.21: The Stroop test and digital span test (Dong-Kyun, Min-Ho, John & Seong-Whan, 2019).

Next, the second important element is the virtual environment. There is a study mentions that the effect of virtual environment training has more effectiveness than the real environment. They used the Stroop test and digit span test as the result for this study which is shown in *Figure 2.21*. The participants would need to do these tests before the neurofeedback training. After the participants have taken the test, they would have neurofeedback training. The neurofeedback training consists of two groups which are virtual environment training and real environment training. The virtual environment training provided a PC racing game and it was a ranking competition between several AI players. For the real environment training, it provided a mini car and a racing track. Both need to maintain high concentration and relaxation to do the training (Dong-Kyun, Min-Ho, John & Seong-Whan, 2019).

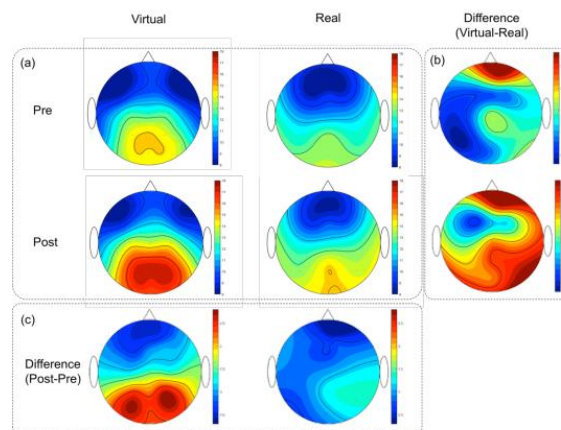


Figure 2.22: The QEEG result of alpha band power (Dong-Kyun, Min-Ho, John & Seong-Whan, 2019).

Table 2.4: The amount of improvement for each indicator of the virtual group and real group (Dong-Kyun, Min-Ho, John & Seong-Whan, 2019).

Indicator		Virtual group			Real group		
EEG	Alpha band power	Frontal	Parietal	Occipital	Frontal	Parietal	Occipital
		8.6%	13.3%	17.5%	8.1%	9.5%	8.7%
Stroop test	Congruent	10.6%			7.0%		
	Incongruent	10.5%			8.8%		
	Control	7.0%			5.9%		
Digit span test	Forward	-0.7%			3.7%		
	Backward	14.7%			12.1%		
Mean		10.2%			8.0%		

As the results show in *Figure 2.22* and *Table 2.4*, the virtual environment has more improvement than the real environment. All the results have shown more improvement in the virtual environment except for the forward digit span test. The reason that the virtual environment has more improvement is the real environment has hardware limitations, it can't provide competition like the AI players. The participants have more interest and motivation in a virtual environment by providing the AI players with competition and a real-time rewards system during the gameplay. So, the virtual environment is one of the important elements that should include in the neurofeedback system (Dong-Kyun, Min-Ho, John & Seong-Whan, 2019).



Figure 2.23: The 2D game stimulus content (2D-GSC) (Yasir, Syed, Syed, Muhammad, Syed, 2019).



Figure 2.24: The 3D game stimulus content (3D-GSC) (Yasir, Syed, Syed, Muhammad, Syed, 2019).

Lastly, the third important element in the BCI system in neurofeedback is the 3D stimulus. There is one study that researches the effect of neurofeedback 2D and 3D stimulus content on stress mitigation. The study is to increase the alpha asymmetry of stress mitigation. They measured the pre-Frontal electrodes which are Fp1 and Fp2 in this experiment. In this experiment, they divided into two groups which are group 1 (G1-NFT) for the 2D stimulus and group 2 (G2-NFT) for the 3D stimulus. Both were using the game stimulus for the neurofeedback training. The 2D and 3D game stimulus content are shown in *Figure 2.23* and *Figure 2.24* (Yasir, Syed, Syed, Muhammad, Syed, 2019).

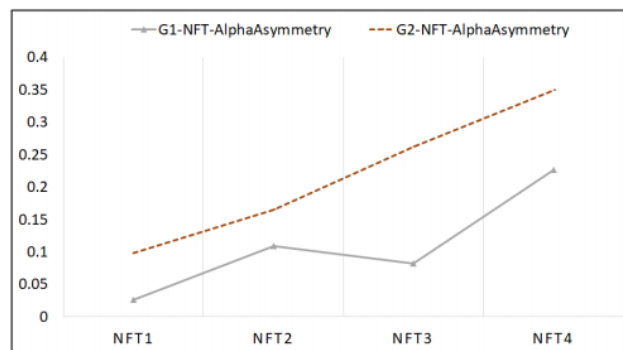


Figure 2.25: The mean value of prefrontal alpha asymmetry for G1-NFT and G2-NFT (Yasir, Syed, Syed, Muhammad, Syed, 2019).

In the result shown in *Figure 2.25*, group 2 used 3D game stimulus content as the neurofeedback has more prefrontal alpha asymmetry than the 2D game stimulus content in group 1. The 3D game stimulus would have more interest than the 2D game stimulus. Other reasons for these results are the 3D stimulus game has high difficulty and complexity than the 2D stimulus game and the participants have to receive more information to make decisions in the 3D game. Thus, the brain would have better practice when playing the 3D game (Yasir, Syed, Syed, Muhammad, Syed, 2019).

2.10. Summary

The brain is a complex and unique organ. Research on the brain is still a very popular topic nowadays. The different parts of the brain have different functions and they have a relationship with each other. If any parts have any issue or damage, it would affect the people in their daily life or even serious would become stroke, paralyze or lost their life.

The brain signal is the result of the amount of postsynaptic potential being simultaneous and in the same direction and it can be measured by the EEG. The different areas of the brain will have different brainwaves and event-related potential. These brain signals and the event-related potentials will help the scientists know the brain working principles, diagnose brain diseases and enhance the functionality of the brain.

The BCI is a device that can help scientists to know about the brain. It is a device that can connect the communication between the brain and the computer. The common BCI electrodes placement used is the international 10/20 system. It is the international system that unified the placement of the electrodes. The system follows the distance between electrodes needs to have 10% or 20% from the total distance from nasion to theinion. There is also another system called the 10/10 and 10/5 system too. It is just to reduce the distance between electrodes to place more electrodes.

In the EEG recording, the EEG signal will contaminate the artifacts. There are a few types of artifacts such as EOG, EMG, ECG, and technical artifacts. Due to artifacts will reduce the accuracy of the EEG signal, therefore pre-processing is needed in EEG recording or BCI to remove artifacts. There are many methods to perform artifact removals such as ICA, regression or adaptive filter, Wavelet transform, and more. In these methods, the ICA is one of the methods that can perform blind source separation. This method separates the independent signals and noise to perform artifact removal. Another method of artifact removal is called the regression method. This method uses the reference signal to cancel the unwanted noise. The difference between the ICA and regression method is the ICA can be used in the unknown mixing process but can't cancel the noise that is not linear. The regression method can remove many types of artifacts but it requires the extra reference signal to perform artifact removal.

There are three important elements to improve the effectiveness of the neurofeedback BCI system which are interactive, virtual stimulus, and the 3D stimulus. The interactive is the information from the BCI and gives data feedback to the person. The data feedback can be text, number, audio, or video. Next, the virtual stimulus is also an important element in the neurofeedback BCI system. In the virtual stimulus, the person can have the competition with the AI and the real-time reward. The real stimulus can't provide these kinds of conditions, so the person may feel boring and can't fully concentrate for a long time. Due to this reason, the real stimulus effectiveness will be weaker than the virtual stimulus. Lastly, the last element is the 3D stimulus. The 3D stimulus has better performance than the 2D stimulus on the neurofeedback BCI system. The brain will gain more complex information from the 3D stimulus, so the participants can have better training in the 3D stimulus.

CHAPTER 3

METHODOLOGY

3.1. Overview

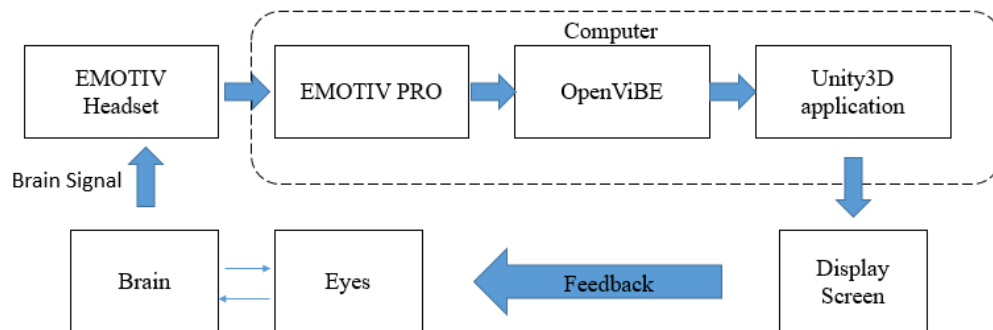


Figure 3.1: The basic flow of the BCI system.

In this project, we will build a neurofeedback BCI system to enhance brain functions such as memory, and concentration and reduce stress. The EMOTIV Insight EEG headset, the software EMOTIV PRO, OpenViBE, MATLAB, and the Unity3D would be used in the project. The EEG headset was used for the brain signals measurement. Firstly, the brain signal of the subject would be collected by the computer and the software EMOTIV PRO will connect to the headset and send the data to the OpenViBE. After that OpenViBE would record and process the brain signal. Next, the OpenViBE would be connected to the application made by Unity3D. The application will receive the signal

from the OpenViBE. Lastly, the real-time result from the application would be feedback to the subject. The process was a closed-loop system which showed in *Figure 3.1*.

This project has two main parts, pre-processing in which the EEG signals were recorded, and artifacts were removed from the data in real-time, and NFT in which the subject received the real-time feedback from its brain. We compared the raw and clean EEG data to show the effect of artifact removal for NFT systems. In the neurofeedback training, Alpha band frequency was used which is 8 to 13 Hz and the difference before and after the neurofeedback training was observed.

3.2. EEG Headset and computer requirement

The EEG headset that would be used in the project is the EMOTIV Insight Headset as shown in *Figure 3.2*. All the details of the EEG headset and computer would be shown in *Table 3.1 and Table 3.2*. The electrode placement of the EMOTIV Insight shows in *Figure 3.3*. The EEG headset needs to connect with the wireless Bluetooth USB. Before using the EEG headset, we needed to put some solution into every electrode to increase the contact quality. The main ingredients of the solution are water and salt.



Figure 3.2: EMOTIV Insight Headset.

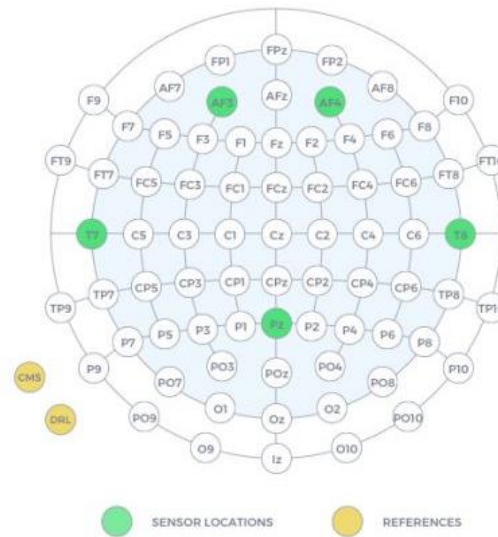


Figure 3.3: The electrode placement of the EMOTIV Insight (EMOTIV, n.d.).

Table 3.1: Technical Specifications for EMOTIV Insight Headset (EMOTIV, n.d.).

Specifications	Details
Sensors	5 channels: AF3, AF4, T7, T8, Pz
Sensors Materials	Hydrophilic semi-dry polymer
Connectivity	Wireless: Bluetooth Low Energy
EEG Sampling Rate	128 samples per second per channel
EEG Resolution	14 bits with 1 LSB = 0.51 μ V
Frequency Response	0.5-43Hz, digital notch filters at 50Hz and 60Hz
Filtering	Built in digital 5th order Sinc filter
Dynamic Range	8400 μ V(pp)
Coupling Mode	AC coupled
Accelerometer	3-axis +/-8g
Gyroscope	3-axis +/-2000 dps
Magnetometer	3-axis +/- 12 gauss
Battery	Internal Lithium Polymer battery 480mAh

Table 3.2: Technical Specifications for the Desktop Computer.

Specifications	Details
CPU	Intel Core i7-6700 CPU @ 3.40GHz
GPU	Nvidia GTX 950
RAM	16 GB
Operating System	Windows 10-64 Bit Home Edition



Figure 3.4: The solution for the headset electrode.



Figure 3.5: The wireless Bluetooth USB.

3.3. EMOTIV PRO

EMOTIV PRO is the software that uses to collect the data from the EMOTIV headset. The version of the EMOTIV PRO that uses in this project is 3.2.3.420. It is freeware that can download through this link: <https://www.emotiv.com/emotiv-launcher/#download>. After connecting the EEG headset to the computer, it can show the information on contact quality and the signal quality for every electrode. **Figure 3.6** shows the contact quality of each electrode and **Figure 3.7** shows the signal quality of each electrode. We need to check overall contact quality is 100% and that the overall signal quality is good before starting the EEG session. It can also show the EEG signal in the time domain as shown in **Figure 3.8**. Next, the Lab Streaming Layer (LSL) is needed to be set up to synchronize streaming across the software. The details of the setting are shown in **Figure 3.9** and **Table 3.3**.

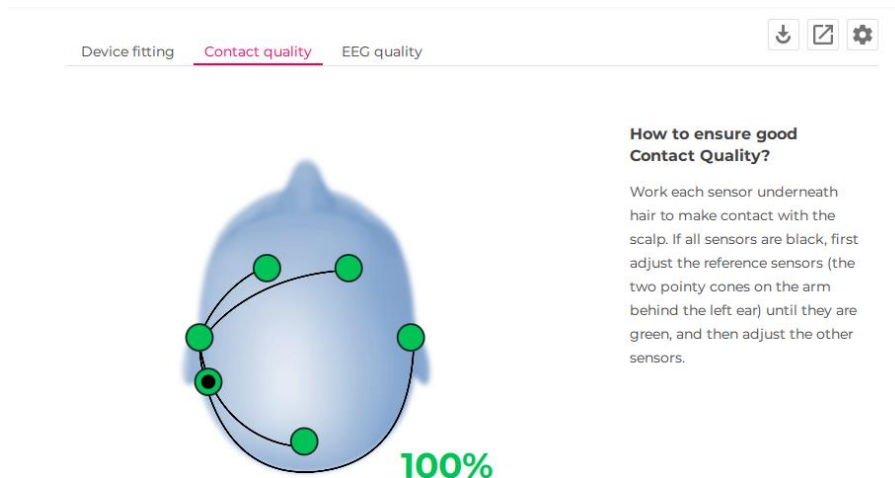
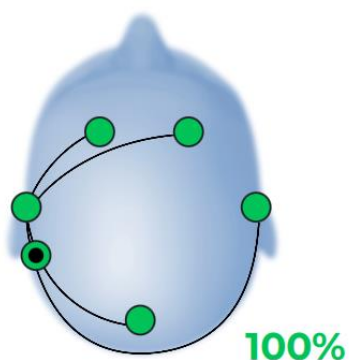


Figure 3.6: The contact quality of each electrode.



How to ensure good EEG Quality?

Continue as for Contact Quality paying special attention to the references. Click on the sensors to compare the current signals with typical good quality EEG signals.

[Learn more](#) 

Figure 3.7: The signal quality of each electrode.

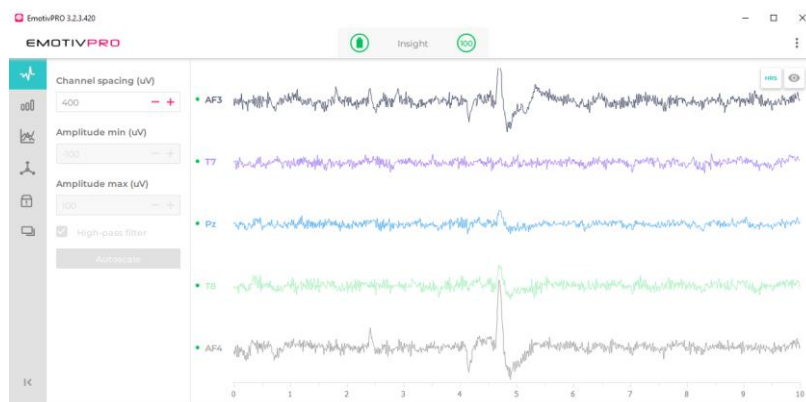


Figure 3.8: The EEG signal in the time-domain.

Data stream

EEG Channels: 10 Sample rate: 128HZ

Motion

Performance Metrics

Contact Quality

EEG Quality

Data format

cf_float32

cf_double64

Transmit type

Sample

Chunk

Start Stop

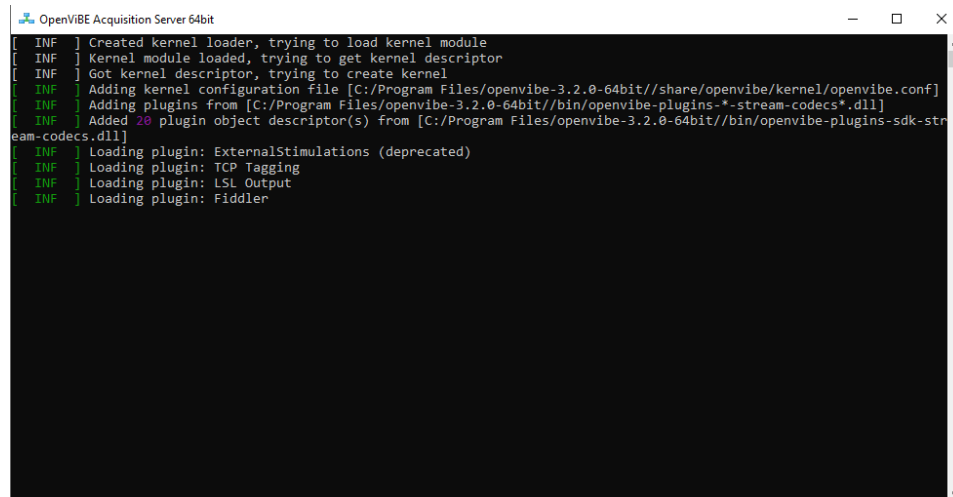
Figure 3.9: The setting of the LSL export in EMOTIV PRO.

Table 3.3: The setting of the LSL in the EMOTIV PRO.

Parameters	Types
Data Stream	EEG
Data Format	cf_float32
Transmit Type	Sample

3.4. OpenViBE

OpenViBE is a software that can collect and process the EEG signal for the BCI system. The version of the OpenViBE that uses in this project is version 3.2.0. It is freeware that can download through this link: <http://openvibe.inria.fr/pub/bin/win64/openvibe-3.2.0-64bit-setup.exe>. It has two parts which are the Acquisition Server and the Designer. The Acquisition Server is the server that makes the connection and received the data from the other software. The setting in Acquisition Server and its driver properties for this project was shown in *Figure 3.11* and *Figure 3.12*.



```

OpenViBE Acquisition Server 64bit
[ INF ] Created kernel loader, trying to load kernel module
[ INF ] Kernel module loaded, trying to get kernel descriptor
[ INF ] Got kernel descriptor, trying to create kernel
[ INF ] Adding kernel configuration file [C:/Program Files/openvibe-3.2.0-64bit//share/openvibe/kernel/openvibe.conf]
[ INF ] Adding plugins from [C:/Program Files/openvibe-3.2.0-64bit//bin/openvibe-plugins-*.stream-codecs*.dll]
[ INF ] Added 20 plugin object descriptor(s) from [C:/Program Files/openvibe-3.2.0-64bit//bin/openvibe-plugins-sdk-stream-codecs.dll]
[ INF ] Loading plugin: ExternalStimulations (deprecated)
[ INF ] Loading plugin: TCP Tagging
[ INF ] Loading plugin: LSL Output
[ INF ] Loading plugin: Fiddler

```

Figure 3.10: The message window for the OpenViBE Acquisition Server.

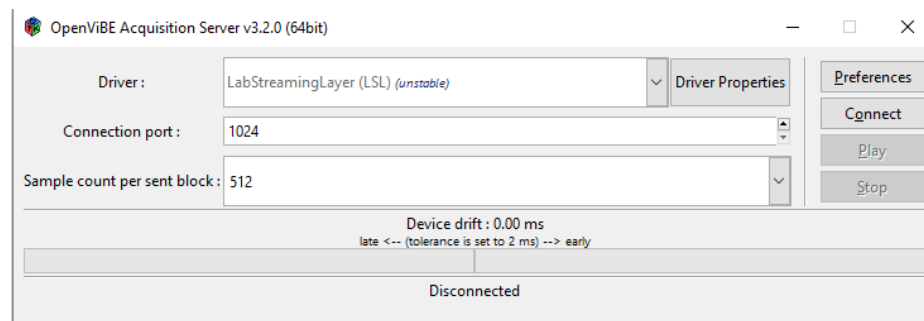


Figure 3.11: The setting in OpenViBE Acquisition Server.

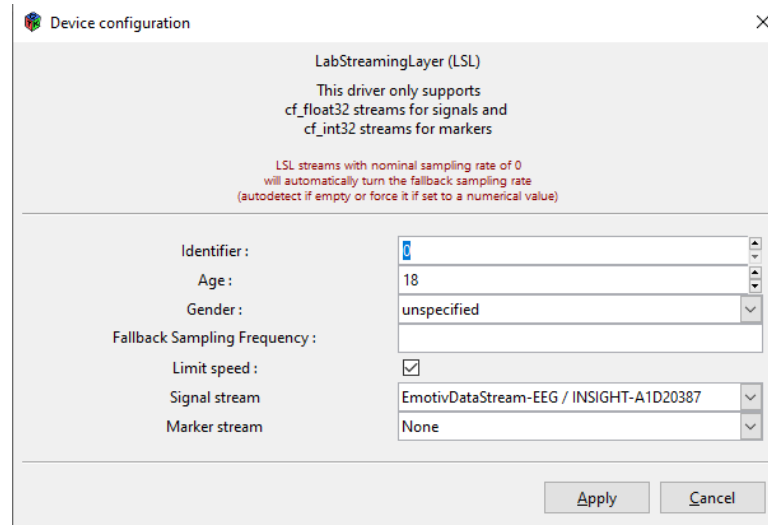


Figure 3.12: The setting of the driver properties.

Next, the OpenViBE Designer is the application that can collect, process, and show the EEG data. It is using the different functional boxes shown in **Figure 3.13** to process the EEG data to the useful information. The overall boxes and connection for the NFT session are shown in **Figure 3.15**. The Acquisition client box is the box that received the data from the Acquisition Server. Next, the channel selector is the box uses to select or reject certain channels from all the channels. In the setting for the channel selector that shows in **Figure 3.16**, the channels that select are from number 4 until number 8. There are 10 channels of data that come from the EMOTIV PRO and channel numbers 1, 2, 9, and 10 are not the EEG signal data, so we just select the 5 channels that consist of the EEG data.

Furthermore, the temporal filter is the box that can perform the four basic frequency filters which are bandpass, band stop, high pass, and low pass filter. There is a temporal filter after the channel selector box because the EEG data needs to limit to a fixed frequency range and confirm the sign of the signal are remain the same compared with the raw signal and the clean signal. The low-cut frequency and high-cut frequency are set to 0.1 to 61 Hz. The MATLAB script box can use the function that writes from MATLAB. Its setting is shown in **Figure 3.17**. The box frequency for the MATLAB script follows the bits in MATLAB, so the MATLAB is using 64-bit and its box frequency will be 64

Hz. The MATLAB executable is the location of the MATLAB application. The MATLAB working directory is the location of the MATLAB files that the program needed to process. There are three MATLAB files required which are Initialize function, the Process function, and the Uninitialized function.

Lastly, the power log signal box is the box that calculates the signal power in the logarithm. Its formula is shown in **Formula 3.1**. The LSL export box is used for the LSL signal export to another software. The signal stream name in the setting puts a name to the LSL import software and it will be easy for the researcher to recognize different streaming data. In this project, the LSL export box from OpenViBE will send the data to the application that build by Unity 3D (Arthur Desbois and Marie-Constance Corsi, 2021) (David Ojeda, 2016).

$$Power_{signal} = \log(1 + mean(x^2)) \quad (3.1)$$

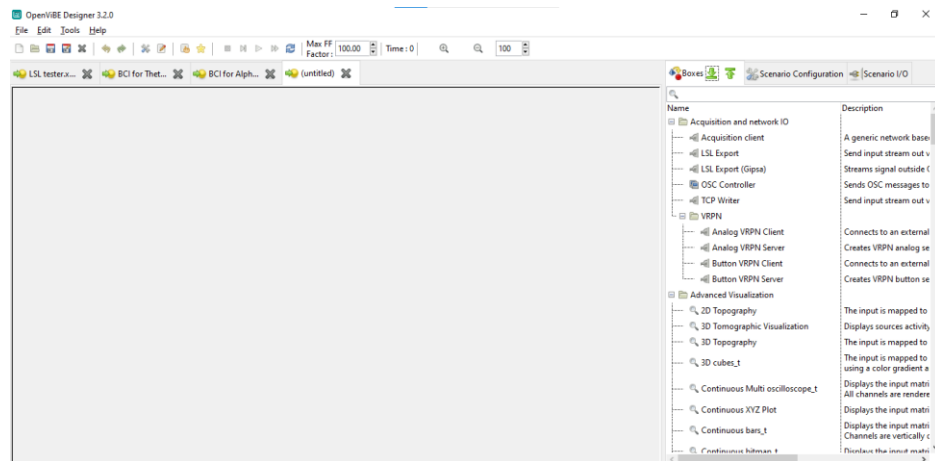


Figure 3.13: The interface of the OpenViBE Designer.

```

OpenViBE Designer 64bit
[INF ] Added 25 plugin object descriptor(s) from [C:/Program Files/openvibe-3.2.0-64bit/bin/openvibe-plugins-sdk-sig-
nal-processing.dll]
[INF ] Added 6 plugin object descriptor(s) from [C:/Program Files/openvibe-3.2.0-64bit/bin/openvibe-plugins-sdk-stim-
ulation.dll]
[INF ] Added 28 plugin object descriptor(s) from [C:/Program Files/openvibe-3.2.0-64bit/bin/openvibe-plugins-sdk-str-
eam-coders.dll]
[INF ] Added 2 plugin object descriptor(s) from [C:/Program Files/openvibe-3.2.0-64bit/bin/openvibe-plugins-sdk-str-
eam-coders.dll]
[INF ] Added 4 plugin object descriptor(s) from [C:/Program Files/openvibe-3.2.0-64bit/bin/openvibe-plugins-sdk-tool-
s.dll]
[INF ] Added 18 plugin object descriptor(s) from [C:/Program Files/openvibe-3.2.0-64bit/bin/openvibe-plugins-signal-
processing.dll]
[INF ] Added 10 plugin object descriptor(s) from [C:/Program Files/openvibe-3.2.0-64bit/bin/openvibe-plugins-simple-
visualization.dll]
[INF ] Added 9 plugin object descriptor(s) from [C:/Program Files/openvibe-3.2.0-64bit/bin/openvibe-plugins-stimulat-
ion.dll]
[INF ] Added 1 plugin object descriptor(s) from [C:/Program Files/openvibe-3.2.0-64bit/bin/openvibe-plugins-streamin-
g.dll]
[INF ] Added 1 plugin object descriptor(s) from [C:/Program Files/openvibe-3.2.0-64bit/bin/openvibe-plugins-tests.dl-
l]
[INF ] Added 2 plugin object descriptor(s) from [C:/Program Files/openvibe-3.2.0-64bit/bin/openvibe-plugins-tools.dl-
l]
[INF ] Added 4 plugin object descriptor(s) from [C:/Program Files/openvibe-3.2.0-64bit/bin/openvibe-plugins-vrpn.dll]
[INF ] Adding metaboxes from [C:/Program Files/openvibe-3.2.0-64bit/share/openvibe/metaboxes/;C:/Users/userR/AppData/Roaming/OpenViBE-3.2.0/metaboxes/]
[INF ] Added 3 metaboxes from [C:/Program Files/openvibe-3.2.0-64bit/share/openvibe/metaboxes/]
[INF ] Added 0 metaboxes from [C:/Users/userR/AppData/Roaming/OpenViBE-3.2.0/metaboxes/]
[INF ] Initialization took 2086 ms

```

Figure 3.14: The message window for the OpenViBE Designer.

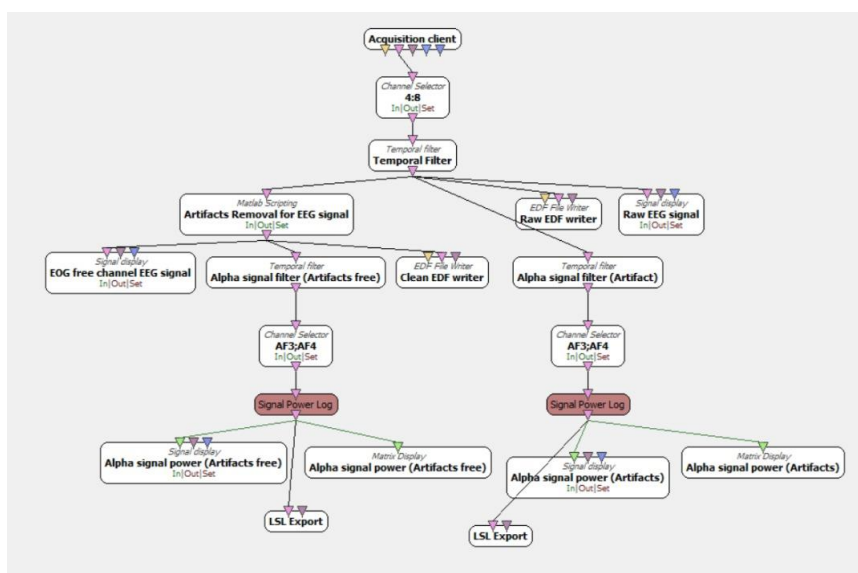


Figure 3.15: The boxes and the connection in the OpenViBE Designer for the NFT.

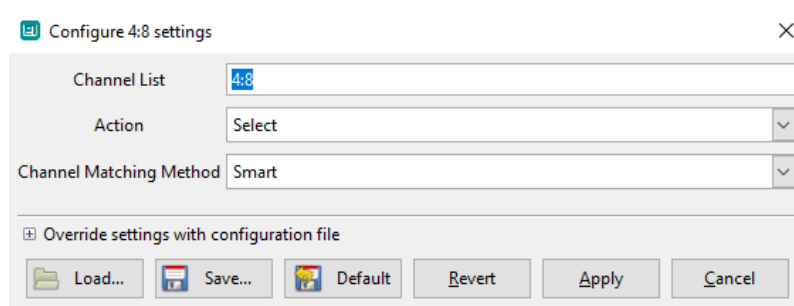


Figure 3.16: The setting for the channel selector.

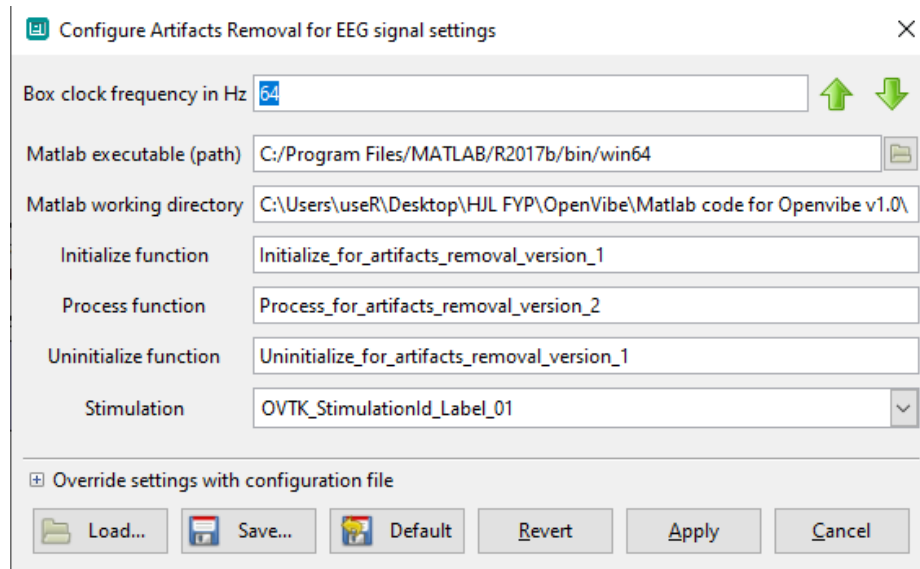


Figure 3.17: The setting of the MATLAB scripting.

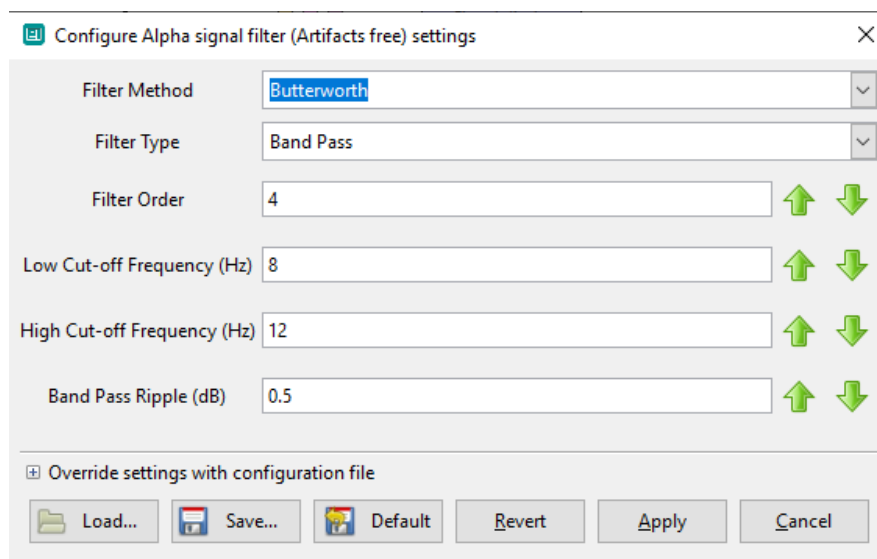


Figure 3.18: The setting for the temporal filter in Alpha band frequency.

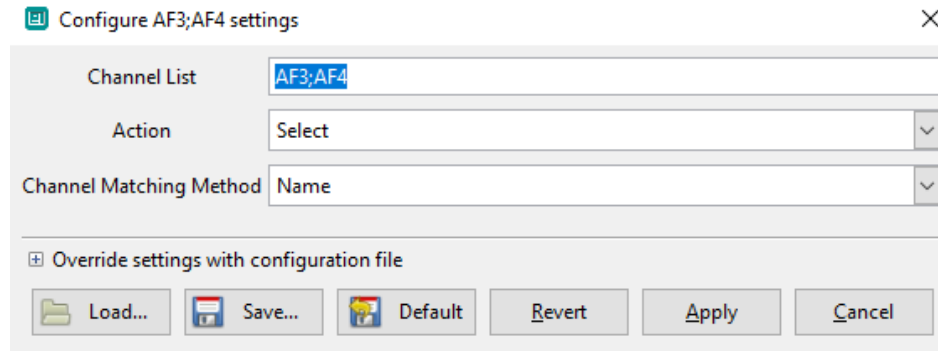


Figure 3.19: The setting for the channel selector that chooses AF3 and AF4 channels.

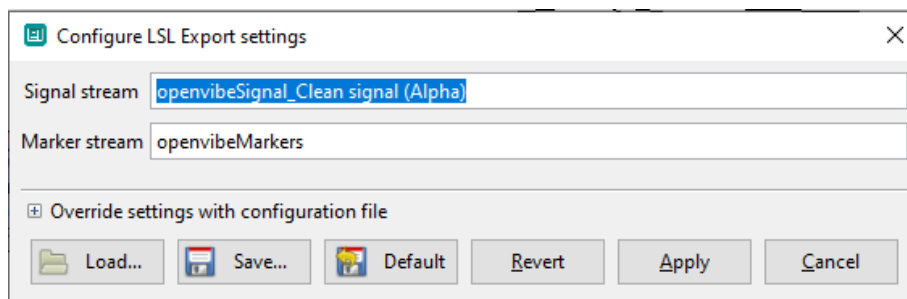


Figure 3.20: The setting of the LSL export.

3.5. MATLAB for OpenViBE scripting

MATLAB is a programming and numerical computing platform that millions of engineers and scientists use to analyze data, design algorithms, and build models. In our project, the MATLAB version that using is R2017b. There are three MATLAB files required which are Initialize function, the Process function, and the Uninitialized function. The Initialize function is the function that needs to proceed before starting to record the EEG signal and the Uninitialized function is the function that needs to proceed after the EEG signal was recorded. The Process function is the function that needs to proceed when the EEG signal was recorded and it also includes the MATLAB codes that have the artifact removal. All the MATLAB coding for the OpenViBE scripting is shown in *Appendix A* (Ibonnet, 2011).

3.6. Unity3D

Unity3D is a freeware that can make 3D games. The version of the Unity3D that uses in this project is version 2020.3.25f1 and it can download through this link: <https://unity.com/download>. It is using the coding C# for all the objects controlled. Before using Unity3D, it needs to create a new project in the Unity Hub as shown in *Figure 3.21*. Next, it will show the empty project for the program as shown in *Figure 3.22*. In this project, we will use the scenes and the C# scripts files for the LSL data receiver that was downloaded from the Git Hub and the link is <https://github.com/Emotiv/labstreaminglayer>.

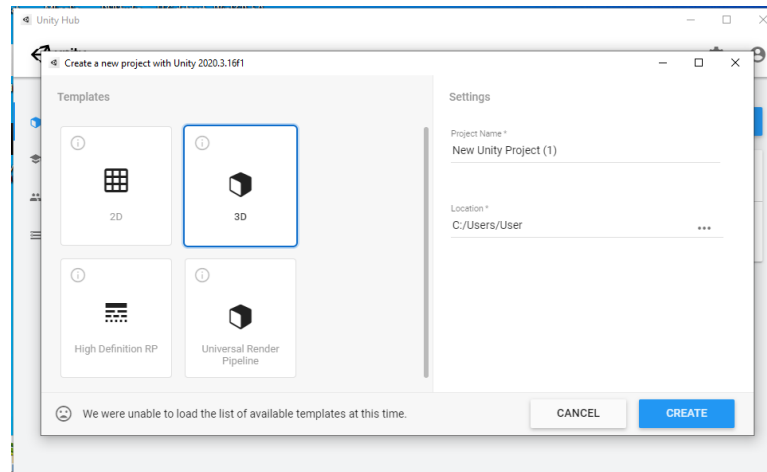


Figure 3.21: The window of creating a new project.

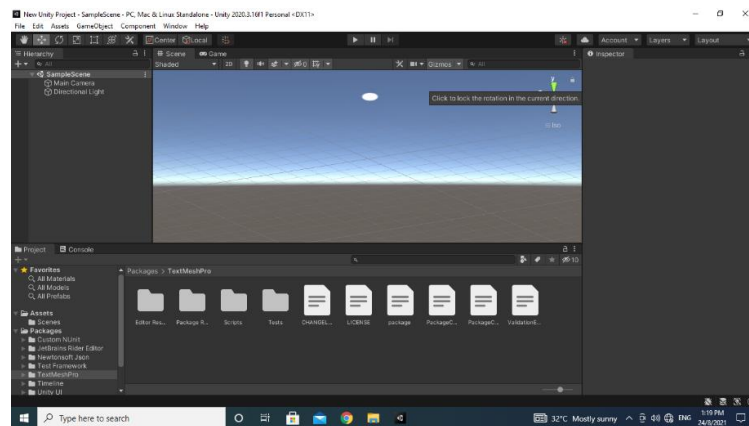


Figure 3.22: The interface of the Unity3D.

In the downloaded files, they provide two example scenes which are the LSL data receiver and LSL data sender. The LSL data receiver will use in the project and its prototype interface is shown in *Figure 3.23*. It can show the stream name, device ID, number of channels, header names, and the data value. Next, we make some changes from the prototype version and add a green bar that will slide by following the value as shown in *Figure 3.24* (Bernard Polidario, 2021). Its value is the mean of all the channels. After all the design and the C# script of the scene were done, the application was built by using the built setting shown in *Figure 3.25*. The interface of the LSL data receiver application shows in *Figure 3.27*.

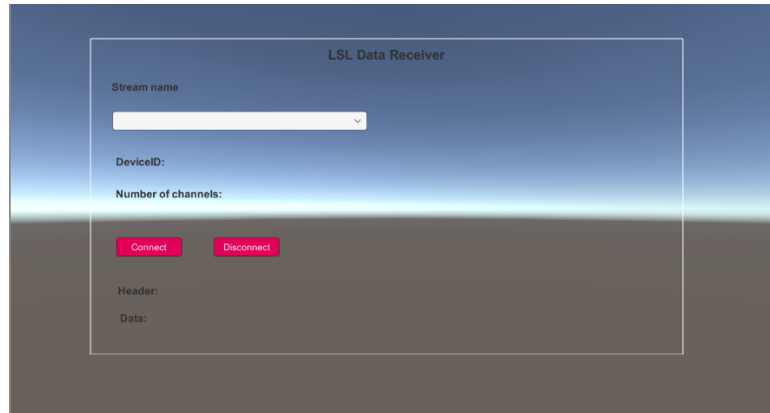


Figure 3.23: The example scene for the LSL data receiver.

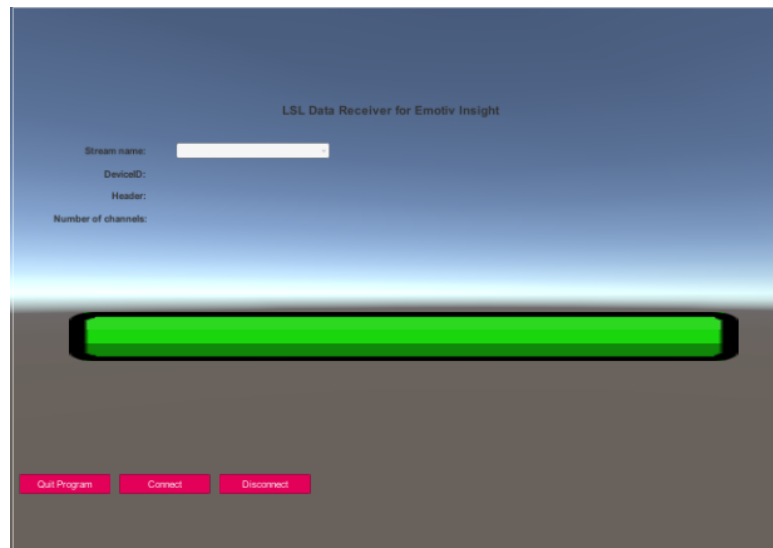


Figure 3.24: The scene for the LSL data for the project.

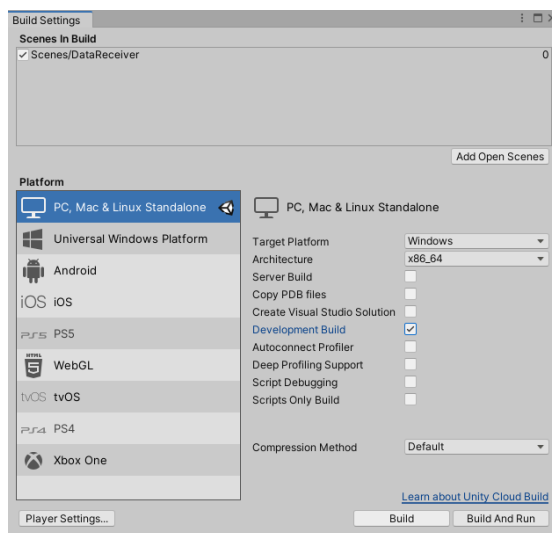


Figure 3.25: The build setting of the Unity3D.

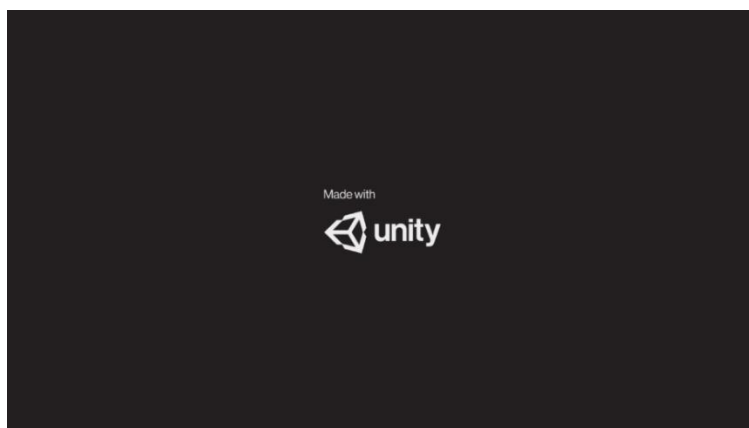


Figure 3.26: The logo of unity when entering the program.

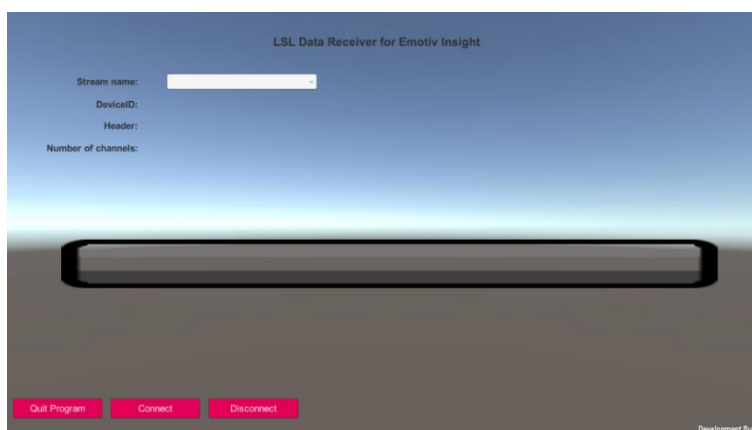


Figure 3. 27: The interface of the LSL data receiver program.

3.7. Neurofeedback training



Figure 3.28: The way of wearing the headset.

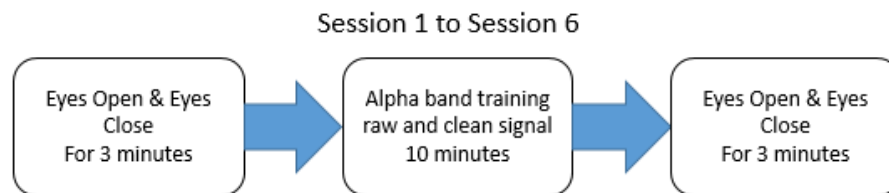


Figure 3.29: The whole process of NFT training.

In this project, we have 6 subjects aged between 23 and 28 who have done the neurofeedback training. The training consists of 6 sections and is shown in **Figure 3.29**. Resting-state, eyes open, and eyes closed EEG data was recorded for three minutes each in the first and last session. In each session, every subject was required to perform two 10 minutes of NFT, one with the raw signal and another one with the clean signal. There was only one session each day. The project was explained to each subject before session 1 and a consent form was signed by the subject. Before starting the training, the subjects need to wear the EEG headset. The preparation process consumes about 3 to 5 minutes. The subjects just needed to sit on the chair and watch the screen that shows the alpha band power using the LSL data program for 10 minutes for the neurofeedback training.



Figure 3.30: The neurofeedback training.



Figure 3.31: The neurofeedback training.

3.8. MATLAB for data analysis

After collecting all the EEG data from the subjects, we will analyze the EEG data by using MATLAB. There is a MATLAB program that can analyze EEG data in offline called EEGLAB. It can be downloaded from the link: <https://sccn.ucsd.edu/eeglab/download.php>. It analyses EEG signal data in .set format and due to our recorded EEG signals being all saved in the .edf format, so they need to convert it to .set format before analyzing. The parameters that will be analyzed from the EEG signals are the correlation with the raw and clean EEG signals, root means square error (RMSE) with the raw and clean EEG signals, and the Alpha power of the EEG signals. The MATLAB scripts for data analysis are shown in *Appendix B*.

3.9. Budget

The budget of using in this project is shown in *Table 3.4*. The total cost uses in this project is about RM 130.41. The cost mainly comes from the purchase EMOTIV student package for the LSL function in EMOTIV PRO. Other items have not been spent at any cost.

Table 3.4: The budget of this project.

Items	Amount (RM)	Notes
Emotiv Insight headset	0.00	It is borrowed from Dr. Nisar and its actual price is about \$ 499.
PC	0.00	It is borrowed from Dr. Nisar.
EMOTIV PRO	0.00	It is freeware.
EMOTIV PRO with LSL license	260.82	It needs to purchase the student package using the function. It needs to pay each month \$ 29.
OpenViBE	0.00	It is freeware.
Unity3D	0.00	It is freeware. If the user is earning over certain money, then it needs to upgrade to Unity Professional to pay for each month.
MATLAB	0.00	It is using the student license or else it needs to pay for each month.
Total	260.82	

CHAPTER 4

RESULT AND DISCUSSION

4.1. Artifact removal by using ICA-REG

There are many methods to perform artifact removal in EEG. The artifact removal is not only limited to using a single method but also can perform in combination to have a better performance. The ICA-REG method is the combination of the ICA method and the Regression method. It first performs the ICA in the raw EEG signals and selects the artifactual independent components. After that, it uses the artifactual independent components as a reference to perform the Regression method.

4.1.1. The working of ICA-REG

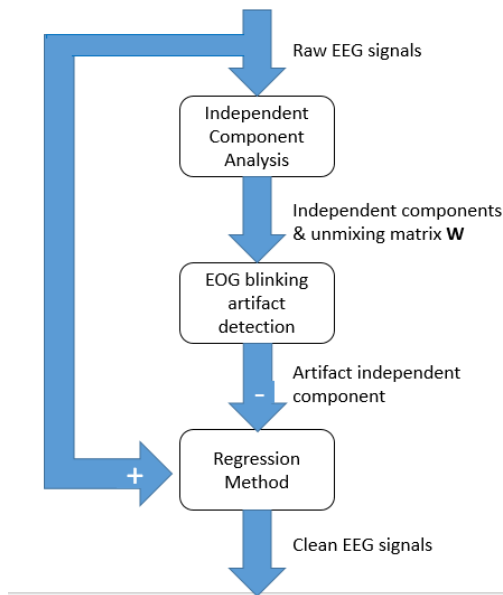


Figure 4.1: The whole process of ICA-REG.

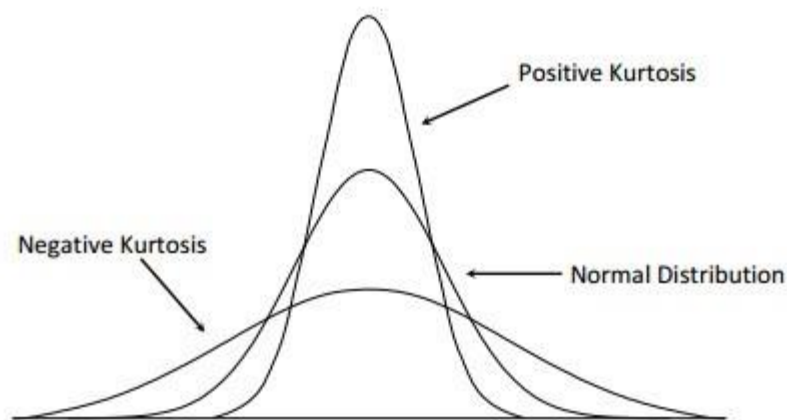


Figure 4.2: The kurtosis compares with the normal distribution (Misha Sv, 2021).

The whole process of the ICA-REG can be categorized into three stages which are Independent Component Analysis, EOG blinking artifact detection, and the Regression method. The first stage of the ICA-REG is to perform Independent Component Analysis in the raw signals to separate them into the independent components and unmixing matrix \mathbf{W} . Next, we use the kurtosis value of the independent components to determine

the artifactual independent components. Kurtosis is a statistical term that describes how much a distribution's tails diverge from the tails of a normal distribution (CFI, n.d.). The formula for the kurtosis is shown in **Formula 4.1**. For finding the artifact EOG IC, these ICs distributions have been standardized to zero-mean and unit standard deviation. If the value of the Z score from ICs are more than 1.64, these ICs will detect as artifactual independent components (Kazi A. and Gleb V. T., 2015).

$$Kurt = \frac{\mu_4}{\sigma^4} \quad (4.1)$$

Where,

μ_4 = fourth central movement

σ = standard deviation

The last stage of the ICA-REG is the Regression method. It uses the detected artifactual IC to remove the EOG blinking noise from the raw signals. **Equation 4.2** shows the formula of the artifactual independent component. Regression analysis was performed at this step to dynamically estimate the weights B_A to be used for artifact removal. It will permit us to build the adaptive spatial filter as shown in **Formula 4.4**. In the end, the adaptive spatial filter is multiplied by the raw signals to get the clean signals.

$$S_A(\tau) = W_A * X(\tau) \quad (4.2)$$

Where,

$S_A(\tau)$ = Artifactual independent component

W_A = Unmixing matrix WA for the artifactual independent components

$X(\tau)$ = EEG data

$$B_A \approx X(\tau) * S_A^T(\tau) * (S_A(\tau) * S_A^T(\tau))^{-1} \quad (4.3)$$

Where,

B_A = Estimated weight

$$F(\tau) = I - X(\tau) * S_A^T(\tau) * (S_A(\tau) * S_A^T(\tau))^{-1} * W_A \quad (4.4)$$

Where,

$F(\tau)$ = adaptive spatial filter

I = Identity matrix

$$X_C(\tau) = F(\tau) * X(\tau) \quad (4.5)$$

Where,

$X_C(\tau)$ = Clean EEG signal

4.1.2. Advantages of using ICA-REG

There are three advantages of using the ICA-REG for artifact removal. The first advantage is that ICA-REG solves the problem on reconstruct the ICs to become clean EEG signals. The ICA method has two main ambiguities which are the sign of the amplitude and the order. If we need to reconstruct the signal, it requires a system that can solve the ambiguities of the ICA and use the free artifactual components to reconstruct the signals. The ICA-REG method uses the artifactual IC as the noise reference of the regression method, so it won't need to worry about the ambiguity issues from the ICA method.

Next, it doesn't need any extra noise reference to perform the artifact removal. The Regression method requires extra noise reference to estimate the weight to deduce the noise from the signal. Unless there have recorded the noise channels or the method that can know actual noise signals, otherwise, it needs to have assumption noise reference to fulfill the requirement. If using the assumption noise reference, its accuracy is based on the similarity of the actual noise and assumption noise. The ICA-REG can solve this kind of problem because the ICA can separate the artifactual component and use it as the noise

reference of the Regression method (Roberto G., Marco M., Federico B., Marco G., and Dante M., 2018).

The last advantage is it can perform online which means in a real-time application. The ICA that uses in the ICA-REG is the fast ICA. The difference between the normal ICA and the fast ICA is the computation of the fast ICA is lower than the normal ICA which requires less memory and more efficiency (Stack Exchange, 2017). The classical regression method, it isn't used the spatial adaptive filter to cancel the noise which makes the computation very expensive and not available for the BCI application. The ICA-REG method uses the spatial adaptive filter to perform artifact removal, so it will reduce the load of the computation and available for the BCI system.

4.1.3. Result of the ICA-REG

The performance of the artifact removal by using the ICA-REG is shown in *Figure 4.3*, *Figure 4.4*, and *Figure 4.5*. The comparison with the raw signal and the clean signal in the channel AF3 and AF4, the spike of the EOG signal was canceled out. The spike is the eyes blinking or eyes movement from the subject. It would produce the EOG noise to contaminate the EEG signal. After performing the ICA-REG, the EOG noise was removed from the EEG signal.

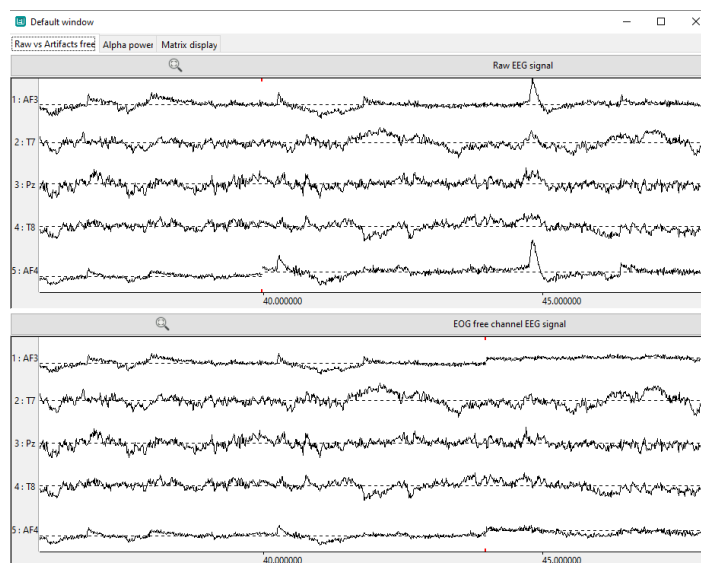


Figure 4.3: The raw EEG and the EOG free EEG signal.

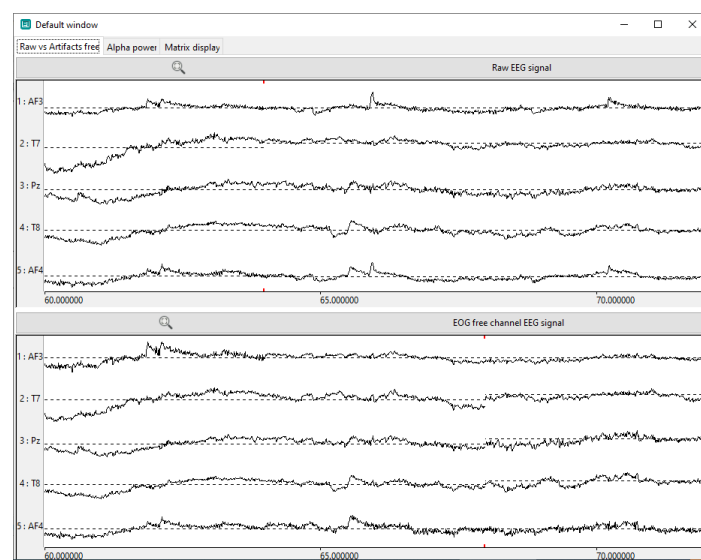


Figure 4.4: The raw EEG and the EOG free EEG signal 2.

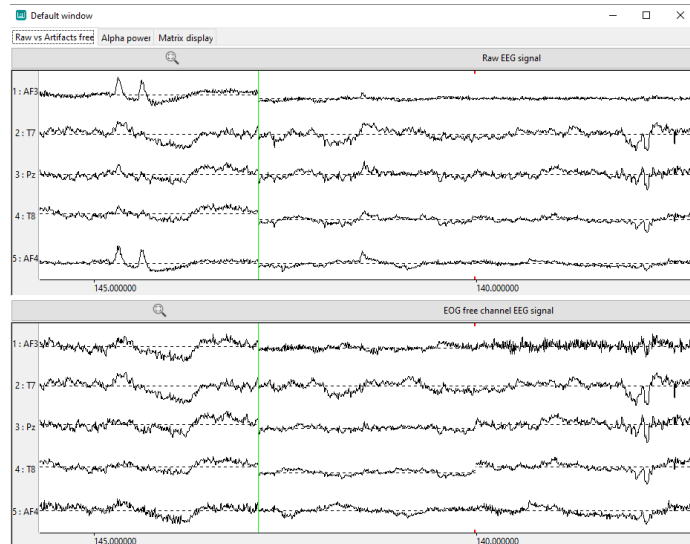


Figure 4.5: The raw EEG and the EOG free EEG signal 3.

4.2. Data Analysis from the NFT training

The parameters that are used in the data analysis of NFT training are the correlation, root mean square error, and the Alpha band power of EEG signal from every session. The correlation and RMSE are used for checking the similarity of the raw signal and the clean signal which means they prove that the training is followed the procedure. Another application for these two parameters is to check the performance of artifact removal. Next, the Alpha band power is to observe the difference in results before and after NFT training.

4.2.1. Correlation

The correlation is the weight of the relationship between the two variables or the signals which means the similarity of these signals. There is a high similarity if the value of correlation is high too. The formula is shown in *Equation 4.6*. Its range can only be within 1 until -1. If the correlation is more than zero, then it is a positive correlation. On the opposite side, if it is less than zero, it is a negative correlation (Steven N., 2021). In signal processing, the value of the positive correlation and negative correlation shows how similar the two variables are. The difference between them is the positive correlation has the same sign but the negative correlation has the negative sign.

$$correlation = \frac{\Sigma(x_i - \bar{x})(y_i - \bar{y})}{\sqrt{\Sigma(x_i - \bar{x})^2 \Sigma(y_i - \bar{y})^2}} \quad (4.6)$$

Where,

x_i = values of the x -variable in a sample

\bar{x} = mean of the value of the variables x

y_i = values of the y -variable in a sample

\bar{y} = mean of the value of the variables y

In our data analysis, we compare the correlation between the raw signal and the clean signal in every session. The correlation in the session before training and after training has a high correlation which is at least have 0.8895. The high correlation in the session before training and after training is because we record the raw and clean signal at the same time. The only difference between the two signals is that one has the EOG artifacts while the other is the artifact-cleaned signal. Next, the correlation in the NFT training sessions has a very small value which is between -0.01 and 0.01. The reason for the low correlation in the NFT training session is we have trained subjects in two-time frames of 10 minutes. Furthermore, the high correlation in the session before training and after training means that the performance of the artifact removal is good. It still has high

similarity after performing the artifact removal which means the user data didn't wipe out after performing the artifact removal.

Table 4.1: The correlation of the EEG recorded signal from Subject 1 to Subject 3.

Section	EEG recorded signal	Subject 1	Subject 2	Subject 3
Before training	Eyes Open 3 minutes	0.9911	0.8895	0.9916
	Eyes Close 3 minutes	0.9963	0.9979	0.9962
1	Alpha Band 10 minutes	-0.0046	0.0628	-0.0141
2	Alpha Band 10 minutes	-0.0049	0.0447	0.0091
3	Alpha Band 10 minutes	-0.0304	0.0421	0.0163
4	Alpha Band 10 minutes	-0.0030	-0.0081	-0.0447
5	Alpha Band 10 minutes	0.0178	-0.0132	-0.0045
6	Alpha Band 10 minutes	0.0468	0.0021	0.0181
After training	Eyes Open 3 minutes	0.9582	0.9313	0.9746
	Eyes Close 3 minutes	0.9541	0.9580	0.9791

Table 4.2: The correlation of the EEG recorded signal from Subject 4 to Subject 6.

Section	EEG recorded signal	Subject 4	Subject 5	Subject 6
Before training	Eyes Open 3 minutes	0.9912	0.9689	0.9837
	Eyes Close 3 minutes	0.9779	0.9684	0.9992
1	Alpha Band 10 minutes	0.0397	0.0083	0.0044
2	Alpha Band 10 minutes	-0.0092	0.0557	0.0202
3	Alpha Band 10 minutes	-0.0272	-0.0127	-0.0273
4	Alpha Band 10 minutes	-0.0115	0.0014	0.0186
5	Alpha Band 10 minutes	-0.0097	0.0129	0.0394
6	Alpha Band 10 minutes	-0.0070	0.0408	-0.0085
After training	Eyes Open 3 minutes	0.9758	0.9947	0.9154
	Eyes Close 3 minutes	0.9944	0.9591	0.9812

4.2.2. Root Mean Square Error

Root Mean Square Error (RMSE) is a parameter that calculates the standard deviation of the residuals from the raw and clean signal. It is to check how far the clean signal is from the raw signal. The smaller value in RMSE, the better result of the quality of the artifact removal in EEG signals (Statistic How To, n.d.). The formula shows in *Formula 4.7*. In our project, the RMSE is used to check the quality of the clean signal. *Table 4.3* and *Table 4.4* show that the RMSE in session before training and after training has a very small value. Its range is between 0.0036 and 0.0511. The reason is that we record the raw signal and the clean signal at the same time. The artifact removal was applied to the raw signal to get a clean signal, so it has a small residual compared to the raw signal.

$$RMSE = \sqrt{\frac{\sum_{i=1}^N \|x(i) - y(i)\|^2}{N}} \quad (4.7)$$

Where,

N = number of data point

$x(i)$ = actual variable

$y(i)$ = predict variable

i = variables

Next, the RMSE in NFT training has a higher value compared to the session before training and after training. Its range is between 0.0932 and 0.7128. The results are great because we train the subject twice with raw signal and clean signal. Both are recorded separately. Even though these two signals are recorded separately, the value of RMSE should not be too high. If the value is more than 1 means that the clean signal may be canceled out the useful information by the artifact removal. The results of RMSE in the project are all below 1, so the performance of the artifact removal is considered as good.

Table 4.3: The RMSE of the EEG recorded signal from Subject 1 to Subject 3.

Section	EEG recorded signal	Subject 1	Subject 2	Subject 3
Before training	Eyes Open 3 minutes	0.0222	0.0375	0.0255
	Eyes Close 3 minutes	0.0122	0.0058	0.0095
1	Alpha Band 10 minutes	0.2598	0.2369	0.4115
2	Alpha Band 10 minutes	0.0932	0.2008	0.2696
3	Alpha Band 10 minutes	0.0993	0.4963	0.3619
4	Alpha Band 10 minutes	0.2176	0.1653	0.3306
5	Alpha Band 10 minutes	0.2405	0.2902	0.4701
6	Alpha Band 10 minutes	0.5668	0.1622	0.2785
After training	Eyes Open 3 minutes	0.0400	0.0302	0.0271
	Eyes Close 3 minutes	0.0371	0.0199	0.0174

Table 4.4: The RMSE of the EEG recorded signal from Subject 4 to Subject 6.

Section	EEG recorded signal	Subject 4	Subject 5	Subject 6
Before training	Eyes Open 3 minutes	0.0266	0.0408	0.0102
	Eyes Close 3 minutes	0.0511	0.0376	0.0036
1	Alpha Band 10 minutes	0.5490	0.5546	0.1180
2	Alpha Band 10 minutes	0.3420	0.3881	0.2029
3	Alpha Band 10 minutes	0.6290	0.4185	0.2840
4	Alpha Band 10 minutes	0.2531	0.5518	0.7128
5	Alpha Band 10 minutes	0.1618	0.5685	0.4851
6	Alpha Band 10 minutes	0.3343	0.2473	0.2022
After training	Eyes Open 3 minutes	0.0452	0.0162	0.0427
	Eyes Close 3 minutes	0.0113	0.0554	0.0054

4.2.3. Alpha band power

The Alpha power is the power of the EEG signal in the frequency range between 8 and 13 Hz. The power spectrum density is used to calculate the power of the EEG signals. Its unit in the EEG commonly is the micro-voltage square per unit frequency. In our project, we used alpha band power to determine the effect of the NFT on the cognition of the subjects. *Table 4.5, Table 4.6, and Table 4.7* show the result of the NFT training among the six subjects.

The result shows that the alpha band power is commonly small. Its range is between 4 to 40 μV^2 . The different subjects can generate the different amplitudes of the alpha power because all the brains are unique and complicated. The power in opened eyes and closed eyes data is the baseline data for the EEG research. It is used to determine the subject's performance in the resting state.

Table 4.8 shows that Subject 1 and Subject 2 have a significant increase in alpha power after NFT training. The NFT training can improve the cognition performance of the human by observing the Alpha power (Rab N., Humaira N., Vooi V. Y. and Chi-Ti T., 2022), so both subjects improve their cognition performance. Next, Subject 3 and Subject 5 don't have too much change in the training. These results show that Subject 3 and Subject 5 do not have enough sessions of NFT training to improve their cognition performance or these subjects might be non-learners in this NFT. Subject 4 has a significant improvement in eyes opened Alpha power but similar in eyes-closed Alpha power after training. This means that the subject has shown some improvement in cognition performance after the training. Lastly, Subject 6 has similar eyes opened Alpha power and reduced the eyes closed Alpha power after training. The reason for the result from Subject 6 is the subject may not have not enough sleep or was already tired when recording the EEG signal.

Table 4.5: The Alpha power of the EEG recorded signal from Subject 1 and Subject 2.

Session	EEG recorded signal	Subject 1		Subject 2	
		Raw signal ($\mu V^2/Hz$)	Clean signal ($\mu V^2/Hz$)	Raw Signal ($\mu V^2/Hz$)	Clean signal ($\mu V^2/Hz$)
Before training	Eyes Open 3 minutes	8.1737	8.1431	7.4228	5.8557
	Eyes Close 3 minutes	27.7678	27.6055	9.9830	9.8765
1	Alpha Band 10 minutes	9.2839	27.1529	7.5848	7.6877
2	Alpha Band 10 minutes	4.6399	4.6140	6.8624	10.7328
3	Alpha Band 10 minutes	4.9258	5.5447	8.0796	9.5008
4	Alpha Band 10 minutes	11.8518	10.1957	11.0025	13.8684
5	Alpha Band 10 minutes	22.6859	17.0248	15.4802	15.4851
6	Alpha Band 10 minutes	27.8724	21.2477	15.9772	15.1186
After training	Eyes Open 3 minutes	30.6118	27.3085	18.0768	17.0530
	Eyes Close 3 minutes	32.8816	33.1807	19.3027	17.8215

Table 4.6: The Alpha power of the EEG recorded signal from Subject 3 and Subject 4.

Session	EEG recorded signal	Subject 3		Subject 4	
		Raw signal ($\mu V^2/Hz$)	Clean signal ($\mu V^2/Hz$)	Raw Signal ($\mu V^2/Hz$)	Clean signal ($\mu V^2/Hz$)
Before training	Eyes Open 3 minutes	11.6640	12.0992	7.8414	8.8046
	Eyes Close 3 minutes	28.0531	27.8804	18.1917	20.3920
1	Alpha Band 10 minutes	14.9655	15.9672	20.0117	25.2314
2	Alpha Band 10 minutes	18.5624	19.0177	14.6227	28.4282
3	Alpha Band 10 minutes	27.1668	35.5956	16.4684	22.8705
4	Alpha Band 10 minutes	21.5831	32.9902	18.8385	23.3701
5	Alpha Band 10 minutes	20.8128	22.2743	7.8005	14.1202
6	Alpha Band 10 minutes	21.5324	19.3369	13.2643	23.8395
After training	Eyes Open 3 minutes	10.8674	11.3938	21.3658	21.5489
	Eyes Close 3 minutes	26.2850	25.8441	18.7126	18.7624

Table 4.7: The Alpha power of the EEG recorded signal from Subject 5 and Subject 6.

Session	EEG recorded signal	Subject 5		Subject 6	
		Raw signal ($\mu V^2/Hz$)	Clean signal ($\mu V^2/Hz$)	Raw Signal ($\mu V^2/Hz$)	Clean signal ($\mu V^2/Hz$)
Before training	Eyes Open 3 minutes	8.8332	10.5407	11.8936	10.7610
	Eyes Close 3 minutes	15.7532	18.4208	20.8356	20.5842
1	Alpha Band 10 minutes	19.5107	13.9429	16.6726	17.0622
2	Alpha Band 10 minutes	23.7934	13.7006	25.9091	21.2877
3	Alpha Band 10 minutes	21.3274	15.0576	20.7088	25.3905
4	Alpha Band 10 minutes	18.3129	12.7861	12.2219	31.3558
5	Alpha Band 10 minutes	18.1256	15.5223	12.4528	15.5549
6	Alpha Band 10 minutes	7.0749	15.8875	15.7436	17.5221
After training	Eyes Open 3 minutes	9.0981	9.2088	10.0094	10.8105
	Eyes Close 3 minutes	18.5953	19.5626	13.0951	12.8463

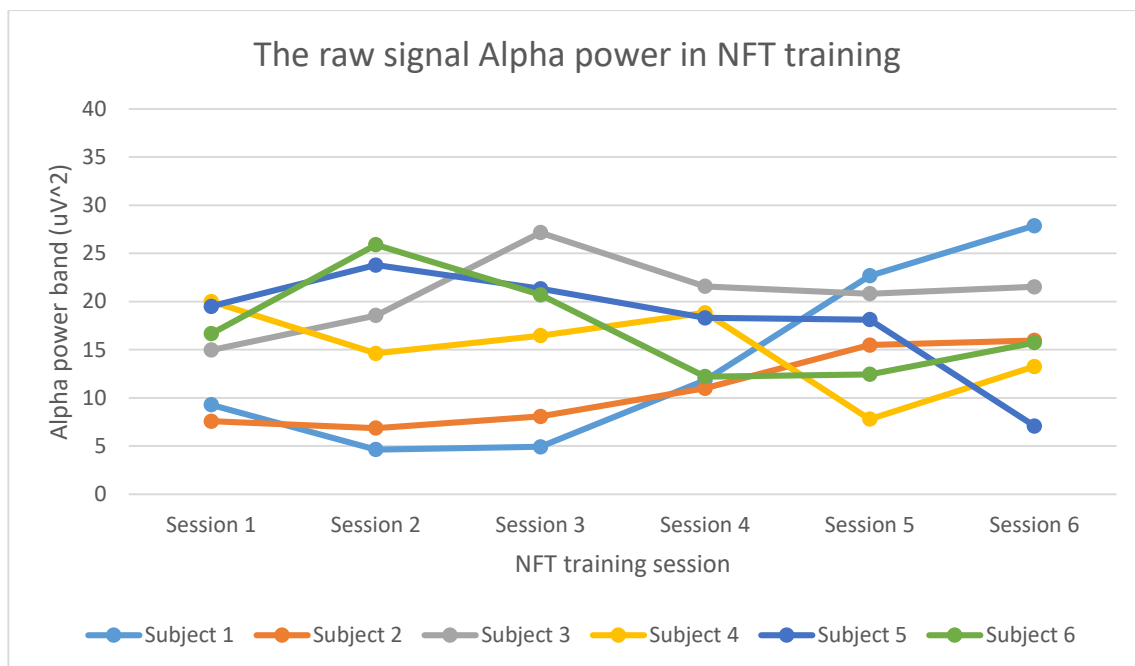


Figure 4.6: The graph of the raw signal Alpha power in NFT training.

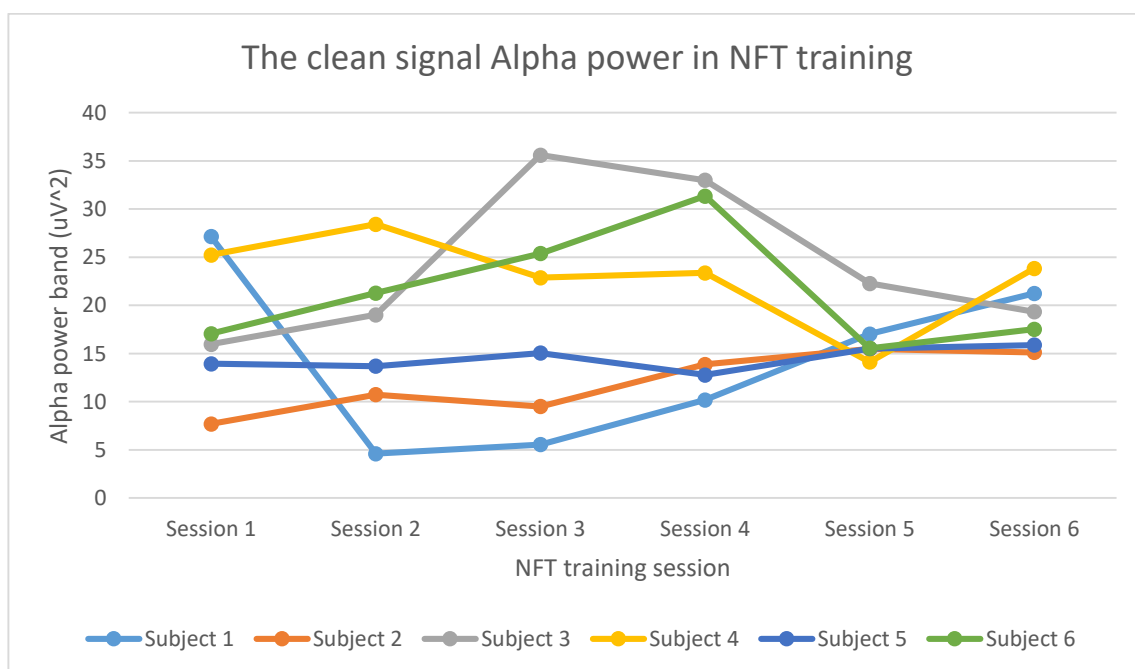


Figure 4.7: The graph of the clean signal Alpha power in NFT training.

Table 4.8: The Alpha power of all subjects in session before training and after training.

Subject		Before training		After training	
		Raw signal ($\mu V^2/Hz$)	Clean signal ($\mu V^2/Hz$)	Raw signal ($\mu V^2/Hz$)	Clean signal ($\mu V^2/Hz$)
Subject 1	Eyes Open	8.1737	8.1431	30.6118	27.3085
	Eyes Close	27.7678	27.6055	32.8816	33.1807
Subject 2	Eyes Open	7.4228	5.8557	18.0768	17.0530
	Eyes Close	9.9830	9.8765	19.3027	17.8215
Subject 3	Eyes Open	11.6640	12.0992	10.8674	11.3938
	Eyes Close	28.0531	27.8804	26.2850	25.8441
Subject 4	Eyes Open	7.8414	8.8046	21.3658	21.5489
	Eyes Close	18.1917	20.3920	18.7126	18.7624
Subject 5	Eyes Open	8.8332	10.5407	9.0981	9.2088
	Eyes Close	15.7532	18.4208	18.5953	19.5626
Subject 6	Eyes Open	11.8936	10.7610	10.0094	10.8105
	Eyes Close	20.8356	20.5842	13.0951	12.8463

CHAPTER 5

RECOMMENDATIONS AND CONCLUSIONS

5.1 Future work and Recommendations

This project can be improved in the future. Firstly, artifact removal applied in this project can only remove EOG removal in the EEG signal. Although the EOG signal is one of the most contaminated artifacts, there are still other artifacts like EMG or ECG signals also can affect the accuracy of the NFT. It can be improved by modifying this method or performing other methods. Next, the computation power of the computer that is used for the BCI system may not enough for the long-time EEG recording. The computer needs to receive EEG data from the headset, process it by using OpenVibe, do feedback on the Unity3D application, and recorded the EEG files at the same time. All these processes would consume a heavy load on the computer and it sometimes may hang when using the BCI system. Therefore, computer up-gradation can improve the BCI system.

Furthermore, the sessions for the NFT training are not enough for this project. The brain is unique for everyone which means the cognition performance is also different for different people. The limited sessions for NFT training may not enough to improve the cognition performance of the subject. NFT training can be improved by increasing the number of sessions from 6 to 10 or even 20. Lastly, the interface of the neurofeedback is boring for the subjects. The attractiveness of the interface can affect the result of the NFT

training. If the interface of the neurofeedback is more interesting, the result of the NFT training might be increased too.

5.2 Conclusion

The acquisition of real-time EEG data and application of pre-processing methods such as signal decomposition and real-time artifact removal has been successfully performed in this project. The BCI system was built which can record the raw signal and remove the artifactual signal for the NFT training. Furthermore, an application in Unity3D was also built for the NFT-BCI system. Finally, the effect of using raw EEG data and online artifact cleaned EEG data for NFT sessions has been compared by the correlation and RMSE. The small value of RMSE and high values of correlation between resting-state raw and cleaned EEG signals indicates that the artifacts were removed. The visual inspection of EEG signals also supports our findings. The Alpha power band also proved that the NFT training can improve cognitive performance. Although we have found out that some subjects could not show any learning after NFT but the alpha power of Resting-State EEG before and after EEG training indicates that there is some learning due to NFT. Finally, in comparison to NFT using raw signals and cleaned signals, no significant change was founded which might be because of a very small number of subjects and sessions as well as the only artifact removed was EOG while other artifacts were still in the recorded EEG data.

REFERENCE

Adaptive Filters, 2015. [video] Churchill CompSci Talks.

Available at: <<https://www.youtube.com/watch?v=yDouldS2g38>>

[Accessed 11 April 2022]

Anping Huang, Xinjiang Zhang, Runmiao Li and Yu Chi, 2018. *Memristor Neural Network Design*. [online]

Available at:

<https://www.researchgate.net/publication/324229756_Memristor_Neural_Network_Design/download>

[Accessed 16 August 2021]

Arefa Cassoobhoy, MD, MPH, 2020. *Electroencephalograph (EEG)*. [online]

Available at: <<https://www.webmd.com/epilepsy/guide/electroencephalogram-eeeg>>

[Accessed 19 June 2021]

Arthur Desbois and Marie-Constance Corsi, 2021. *BRAIN-COMPUTER INTERFACE USING OPENVIBE, AN OPEN-SOURCE SOFTWARE PLATFORM*. [online]

Available at: <https://hal.archives-ouvertes.fr/hal-03374960/file/HandsOn_OV_CuttingEEG_2021.pdf>

[Accessed 15 April 2022]

Bernard Polidario, 2021. *Unity Tutorials: How To Make a Health Bar in Unity!*. [online]

Available at: <<https://weeklyhow.com/how-to-make-a-health-bar-in-unity/>>

[Accessed 15 April 2022]

BioNinja, n.d. *Brain Section*. [online]

Available at: <<https://ib.bioninja.com.au/options/option-a-neurobiology-and/a2-the-human-brain/brain-sections.html>>

[Accessed 16 August 2021]

Bit Brain, 2020, *All about EEG artifacts and filtering tools*. [online]

Available at: <<https://www.bitbrain.com/blog/eeg-artifacts>>

[Accessed 9 April 2022]

Catherine, 2014. *High density EEG—What do we have to lose?* [online]

Available at: <<https://www.ncbi.nlm.nih.gov/pmc/articles/PMC4289454/>>

[Accessed 18 August 2021]

Center for Brain, n.d. *What is Neurofeedback?* [online]

Available at: <<https://www.centerforbrain.com/neurofeedback/what-is-neurofeedback/>>

[Accessed 29 June 2021]

CFI, n.d. *Kurtosis*. [online]

Available at: <<https://corporatefinanceinstitute.com/resources/knowledge/other/kurtosis/>>

[Accessed 17 April 2022]

David Ibañez, 2014. *Hans Berger: Lights and Shadows of the Inventor of Electroencephalography*. [online]

Available at: <<https://www.neuroelectrics.com/blog/2014/12/18/hans-berger-lights-and-shadows-of-the-inventor-of-electroencephalography/>>

[Accessed 19 June 2021]

David Ojeda, 2016. *OpenViBE tutorial*. [online]

Available at: <<http://openvibe.inria.fr/openvibe/wp-content/uploads/2016/06/OpenViBE-basics-tutorial.pdf>>

[Accessed 15 April 2022]

Dong-Kyun Han, Min-Ho Lee, John Williamson & Seong-Whan Lee, 2019. The Effect of Neurofeedback Training in Virtual and Real Environments based on BCI. *Institute for Information and Communications Technology Promotion*. [e-journal]

Available through: Universiti Tunku Abdul Rahman Library website

< <https://library.utar.edu.my/>>

[Accessed 21 August 2021]

EMOTIV, n.d. *EMOTIV Insight 2.0 – 5 Channel Mobile Brainwear®* [online]

Available at: < <https://www.emotiv.com/product/emotiv-insight-5-channel-mobile-brainwear/>>

[Accessed 13 April 2022]

Eran Klein and Katherine Pratt, 2017. *Helping or hacking? Engineers and ethicists must work together on brain-computer interface technology*. [online]

Available at: < <https://theconversation.com/helping-or-hacking-engineers-and-ethicists-must-work-together-on-brain-computer-interface-technology-77759>>

[Accessed 19 August 2021]

ERS, 2016. *10-20 system EEG Placement*. [online]

Available at: < <https://www.ers-education.org/lrmedia/2016/pdf/298830.pdf>>

[Accessed 18 August 2021]

Georgia Chronaki, n.d. *Curious Kids: how does our brain send signals to our body?* [online]

Available at: < <https://theconversation.com/curious-kids-how-does-our-brain-send-signals-to-our-body-124950>>

[Accessed 16 August 2021]

Hyunmi Lim & JeongHun Ku, 2018. A Brain–Computer Interface-Based Action Observation Game That Enhances Mu Suppression.

IEEE TRANSACTIONS ON NEURAL SYSTEMS AND REHABILITATION ENGINEERING [e-journal] 26 (12).

Available through: Universiti Tunku Abdul Rahman Library website

< <https://library.utar.edu.my/>>

[Accessed 20 August 2021]

Hyvarinen & Oja, 2000. *Independence Components Analysis: Algorithms and Application.*

[online]

Available at: < <https://www.cs.helsinki.fi/u/ahyvarin/papers/NN00new.pdf>>

[Accessed 31 March 2022]

Ibonnet, 2011. *Tutorial 1: Implementing a signal processing box.* [online]

Available at: < <http://openvibe.inria.fr/tutorial-1-implementing-a-signal-processing-box/>>

[Accessed 15 April 2022]

iMotions, 2015. *Top 6 Most Common Applications for Human EEG Research.* [online]

Available at: <https://imotions.com/blog/top-6-common-applications-human-eeq-research/>>

[Accessed 20 June 2021]

Johns Hopkins Medicine, n.d. *Brain Anatomy and How the Brain Works* [online]

Available at: < <https://www.hopkinsmedicine.org/health/conditions-and-diseases/anatomy-of-the-brain>>

[Accessed 16 August 2021]

Joseph N.Mark, 2010. *Clinical Applications of Brain-Computer Interfaces: Current State and Future Prospects.* [online]

Available at: < <https://www.ncbi.nlm.nih.gov/pmc/articles/PMC2862632/>>

[Accessed 29 June 2021]

JueBin Huang, 2020. *Overview of Cerebral Function*. [online]

Available at: < <https://www.merckmanuals.com/professional/neurologic-disorders/function-and-dysfunction-of-the-cerebral-lobes/overview-of-cerebral-function#v1033994>>

[Accessed 16 August 2021]

Kazi A. and Gleb V. T., 2015. Independent Component Analysis for EOG artifacts minimization of EEG signals using kurtosis as a threshold. *Proceedings of International Conference on Electrical Information and Communication Technology*. [e-journal] EICT 2015, pp137-142.

Available through: < <https://library.utar.edu.my/>> UTAR Library website

[Accessed 9 March 2022]

Lebonheur, n.d. *High Density EEG*. [online]

Available at: < <https://www.lebonheur.org/our-services/neuroscience-institute/advanced-diagnostics-and-testing/high-density-eeeg-/>>

[Accessed 18 August 2021]

Lindsay Patterson, 2009. *Will We Ever Understand Ourselves?* [online]

Available at: < <https://earthsky.org/human-world/neuroscientist-matt-wilsons-revelations-on-the-human-brain/>>

[Accessed 3 August 2021]

Living Well Dallas, 2019. *How a QEEG session can change your life*. [online]

Available at: < https://www.livingwelldallas.com/living_well_dallas_news/how-a-qeeg-session-can-change-your-life/>

[Accessed 5 August 2021]

M. Agustina Garcés Correa and Eric Laciár Leber, 2014. *Noise Removal from EEG Signals in Polisomnographic Records Applying Adaptive Filters in Cascade*. [online] Available at: <https://www.researchgate.net/publication/221913042_Noise_Removal_from_EEG_Signals_in_Polisomnographic_Records_Applying_Adaptive_Filters_in_Cascade> [Accessed 10 April 2022]

Misha Sv, 2021. *Calculate Kurtosis in Python (with Examples)*. [electronic] Available at: <<https://towardsdatascience.com/calculate-kurtosis-in-python-with-examples-pyshark-2b960301393>> [Accessed 17 April 2022]

Muse, 2018. *A Deep Dive into Brainwaves: Brainwave Frequencies Explained* [online] Available at: <<https://choosemuse.com/blog/a-deep-dive-into-brainwaves-brainwave-frequencies-explained-2/>> [Accessed 17 August 2021]

Neuro Health, n.d. *Brainwaves the language*. [online] Available at: <<https://nhahealth.com/brainwaves-the-language/>> [Accessed 18 August 2021]

NeuroTech, n.d. *Intro to Brain Computer Interface*. [online] Available at: <<http://learn.neurotechedu.com/introtobci/>> [Accessed 30 June 2021]

Nitin Sreedhar, 2020. *Our brains remain active all the time, says a new Cambridge study*. [online] Available at: <<https://www.livemint.com/mint-lounge/features/our-brains-remain-active-all-the-time-says-a-new-cambridge-study-11594789903241.html>> [Accessed 3 August 2021]

QEEG support, n.d. *What is qEEG / Brain Mapping?* [online]
 Available at: <<https://qeegsupport.com/what-is-qeeg-or-brain-mapping/>>
 [Accessed 20 June 2021]

Rab N., Humaira N., Vooi V. Y. and Chi-Ti T., 2022. *The Effect of Alpha Neurofeedback Training on Cognitive Performance in Healthy Adults.* [online]
 Available at: < https://mdpi-res.com/d_attachment/mathematics/mathematics-10-01095/article_deploy/mathematics-10-01095.pdf?version=1648538860>\

Robert, n.d. *High-density EEG electrode placement.* [online]
 Available at: < <https://robertoostenveld.nl/electrode/>>
 [Accessed 21 August 2021]

Roberto G., Marco M., Federico B., Marco G. and Dante M., 2018. *Journal of Neural Engineering.* [e-journal] 15(5):056009 <https://pubmed.ncbi.nlm.nih.gov/29952752/>
 [Accessed 9 March 2022]

Rümeysa, Saliha, Fatma, 2020. *The inventor of electroencephalography (EEG): Hans Berger (1873–1941).* [online]
 Available at: < <https://link.springer.com/content/pdf/10.1007/s00381-020-04564-z.pdf>>
 [Accessed 19 June 2021]

Sanjeev N. J. & Dr. Chandashekhar R., 2015. *Blind Source Separation and ICA Techniques: A Review.* [online]
 Available at: < https://www.researchgate.net/publication/265973497_Blind_source_separation_and_ICA_techniques_a_review>
 [Accessed 27 March 2022]

Science Daily, 2019. *Controlling attention with brain waves*. [online]

Available at: <<https://www.sciencedaily.com/releases/2019/12/191204145752.htm>>

[Accessed 18 August 2021]

Shadab Mozaffar & David W. Petr, 2002. *Artifact Extraction from EEG Data Using Independent Component Analysis*. [online]

Available at: <[attachment.googleusercontent.com/attachment/u/0/?ui=2&ik=c35079f309&attid=0.1&permmsgid=msg-](https://mail-attachment.googleusercontent.com/attachment/u/0/?ui=2&ik=c35079f309&attid=0.1&permmsgid=msg-a:r146806923359769402&th=17e9100957a6a8f8&view=att&disp=safe&saddbat=ANGjdJ-f5STolZRtICFPW7uN8oc1Wy2tJ4q-WcdROPmMEZHI3GWYKEURGSkJ62nSXScGndArH6aFDz3_ChYckY2ZW1UQ_GNxPGvn4FZnJXLkN6j1LHrDtNQpcbhj51y4fYgQXb1BWmqHw4trzd5Iv0n8_-JcEKsIEMNVtcUoNFaLjDdOxwI4NCHX7cPsuTG5J2orEtu_OYomm1pVMa3OFYieQowkIN3r7Uf4peRRcfCQte-XHnlFwerQMuUvi219pQ2Tm4z3xRx3dvWHb5XL4bgge7IuZpIWj0UWcKrICLVlvKvANlq-5TJ5uSyiR1khdZZLSVDTxBEc_v0GYq9JiQqKHly9zGc6SxqbDQZBmbjA77pL3qq2FicTO8vDgtG-__vqTCGZfwyAzFEY3K3eFKo205IC65fXyBhAX4aeUt42UASWHlzYOD25LHuGR5exMLuQ7_ZnEkor5R5LMVL2oAJG-8kxhillh-78dwSC1mqrOo7grPNtOT0YdLPCgfQq-ozoNJSUBUKkyg3r6cMxN9eGMXEfN7QuG-KIwETtdOGrU9WDPwQcUiCXltLmmia2WbSHV1WTU_n3fwq4MAwDXUOBmsXRY4CFMItKuiVb1xZTFLhZ8vlpdLXZ7zM6HWYpqrp-WeyA25sG1XXqG743NQCc5qRVywk3zC6yDm19KvB845zjl3sxd2byeXNrBLvk></p>
</div>
<div data-bbox=)

a:r146806923359769402&th=17e9100957a6a8f8&view=att&disp=safe&saddbat=ANGjdJ-f5STolZRtICFPW7uN8oc1Wy2tJ4q-

WcdROPmMEZHI3GWYKEURGSkJ62nSXScGndArH6aFDz3_ChYckY2ZW1UQ_GNxPGvn4FZnJXLkN6j1LHrDtNQpcbhj51y4fYgQXb1BWmqHw4trzd5Iv0n8_-

JcEKsIEMNVtcUoNFaLjDdOxwI4NCHX7cPsuTG5J2orEtu_OYomm1pVMa3OFYieQowkIN3r7Uf4peRRcfCQte-

XHnlFwerQMuUvi219pQ2Tm4z3xRx3dvWHb5XL4bgge7IuZpIWj0UWcKrICLVlvKvANlq-

5TJ5uSyiR1khdZZLSVDTxBEc_v0GYq9JiQqKHly9zGc6SxqbDQZBmbjA77pL3qq2FicTO8vDgtG-

__vqTCGZfwyAzFEY3K3eFKo205IC65fXyBhAX4aeUt42UASWHlzYOD25LHuGR5exMLuQ7_ZnEkor5R5LMVL2oAJG-8kxhillh-

78dwSC1mqrOo7grPNtOT0YdLPCgfQq-ozoNJSUBUKkyg3r6cMxN9eGMXEfN7QuG-

KIwETtdOGrU9WDPwQcUiCXltLmmia2WbSHV1WTU_n3fwq4MAwDXUOBmsXRY4CFMItKuiVb1xZTFLhZ8vlpdLXZ7zM6HWYpqrp-

WeyA25sG1XXqG743NQCc5qRVywk3zC6yDm19KvB845zjl3sxd2byeXNrBLvk>

[Accessed 27 March 2022]

Shailaja Kotte and J R K Kumar Dabbakuti, 2020. *Methods for removal of artifacts from EEG signal: A review*. [online]

Available at: https://www.researchgate.net/publication/347853374_Methods_for_removal_of_artifacts_from

[Accessed 11 April 2022]

Shravani Sur and V.K.Sinha, 2009. *Event-related potential: An overview*. [online]

Available at: <https://www.ncbi.nlm.nih.gov/pmc/articles/PMC3016705/>

[Accessed 19 August 2021]

Sleep Tech Study, 2013. *The International 10/20 System of Electrode Placement*. [online]

Available at: <https://sleeptechstudy.wordpress.com/2013/05/13/the-international-1020-system-of-electrode-placement/>

[Accessed 18 August 2021]

Stack Exchange, 2017. *What is the advantage of FastICA over other ICA algorithms?*.

[online]

Available at: <https://stats.stackexchange.com/questions/260399/what-is-the-advantage-of-fastica-over-other-ica-algorithms>

[Accessed 17 April 2022]

Stat Trek, n.d. *Matrix Rank*. [online]

Available at: <https://stattrek.com/matrix-algebra/matrix-rank.aspx>

[Accessed 11 April 2022]

Statistic How To, n.d. *RMSE: Root Mean Square Error*. [online]

Available at: <https://www.statisticshowto.com/probability-and-statistics/regression-analysis/rmse-root-mean-square-error/>

[Accessed 20 April 2022]

Steven N., 2021. *What Do Correlation Coefficients Positive, Negative, and Zero Mean?*. [online]

Available at: < [The%20covariance%20of&text=The%20correlation%20coefficient%20is%20determined,of%20data%20from%20its%20average.>](https://www.investopedia.com/ask/answers/032515/what-does-it-mean-if-correlation-coefficient-positive-negative-or-zero.asp#:~:text=Calculating%20CF%81,-The%20covariance%20of&text=The%20correlation%20coefficient%20is%20determined,of%20data%20from%20its%20average.></p></div><div data-bbox=)

The%20covariance%20of&text=The%20correlation%20coefficient%20is%20determined,of%20data%20from%20its%20average.>

[Accessed 19 April 2022]

Storti, 2013. *High Density EEG and Electrical Source Imaging*. [online]

Available at: < <https://valli.maths.unitn.it/teaching/Storti.pdf>>

[Accessed 18 August 2021]

Timo Kirschstein and Rudiger Kohling, 2009. What is the Source of the EEG?

CLINICAL EEG and NEUROSCIENCE [e-journal] 40(3)

Available through: Universiti Tunku Abdul Rahman Library website

< <https://library.utar.edu.my/>>

[Accessed 17 August 2021]

Trans Cranial Technologies, 2012. *10/20 System Positioning*. [online]

Available at: < https://www.trans-cranial.com/docs/10_20_pos_man_v1_0_pdf.pdf>

[Accessed 20 August 2021]

Wikipedia, n.d. *Excitatory Postsynaptic Potential*. [online]

Available at: < https://en.wikipedia.org/wiki/Excitatory_postsynaptic_potential>

[Accessed 17 August 2021]

Wikipedia, n.d. *P300 (neuroscience)*. [online]

Available at: < [https://en.wikipedia.org/wiki/P300_\(neuroscience\)](https://en.wikipedia.org/wiki/P300_(neuroscience))>

[Accessed 19 August 2021]

Wikipedia, 2021. *Neurofeedback*. [online]

Available at: <https://en.wikipedia.org/wiki/Neurofeedback#cite_note-Kaiser-27>

[Accessed 23 June 2021]

Wikiwand, n.d. *Hans Berger*. [online]

Available at: <https://www.wikiwand.com/en/Hans_Berger>

[Accessed 19 June 2021]

Xiao Jiang, Gui-Bin Bian and Zean Tian, 2019. *Removal of Artifacts from EEG Signals: A Review*. [electronic print]

Available at: <https://mdpi-res.com/d_attachment/sensors/sensors-19-00987/article_deploy/sensors-19-00987.pdf>

[Accessed 9 April 2022]

Yasir Hafeez, Syed Saad Azhar Ali¹, Syed Faraz, Muhammad Moinuddin, Syed Hasan Adil, 2019. Effect of Neurofeedback 2D and 3D Stimulus Content On Stress Mitigation. *2019 IEEE Student Conference on Research and Development*. [e-journal]

Available through: Universiti Tunku Abdul Rahman Library website

<<https://library.utar.edu.my/>>

[Accessed 21 August 2021]

APPENDICES

APPENDIX A: MATLAB SCRIPT FOR OPENVIBE

```
% Initialize for artifacts removal version 1
% Modified Date: 14th January 2022

function box_out =
Initialize_for_artifacts_removal_version_1(box_in)

    disp('Matlab initialize function has been called.')

    box_in.user_data.trigger_state = false;
    matrix_data_2(1:5)=0;
    box_out = box_in;

end
```

Code Listing 1: The Initialized function.

```

% Process for artifacts removal version 2
% Modified Date: 25th January 2022

function box_out = Process_for_artifacts_removal_version_2(box_in)

    % we iterate over the pending chunks on input 1 (SIGNAL)
    for i = 1: OV_getNbPendingInputChunk(box_in,1)

        % we pop the first chunk to be processed, note that box_in
        is used as the output variable to continue processing
        [box_in, start_time, end_time, matrix_data] =
        OV_popInputBuffer(box_in,1);

        box_in.outputs{1}.header = box_in.inputs{1}.header;

        [ICA, ~, W] = fastica25(matrix_data);
        ICA_transpose=transpose(ICA);
        KS=kurtosis(ICA_transpose);
        fprintf(' KS: %s\n ',KS);
        Zscore=zscore(KS);

        [~, col] = find(Zscore>1.64);
        fprintf(' col: %d\n', col);
        Wa=W(col,:);
        SA = ICA(col,:);

        Final_weight = eye(5)-matrix_data*SA'*((SA*SA')\ Wa);

        CleanSignal=Final_weight*matrix_data;

        % we add the chunk to the signal output buffer. Note that we
        use box_in as the output variable.
        box_in =
        OV_addOutputBuffer(box_in,1,start_time,end_time,CleanSignal);

    end

    % Pass the modified box as output to continue processing
    box_out = box_in;
end

```

Code Listing 2: The Process function.


```
% Uninitialize for artifacts removal version 1
% Modified Date: 14th January 2022

function box_out =
Uninitialize_for_artifacts_removal_version_1(box_in)
    disp('Matlab uninitialize function has been called.')

    box_out = box_in;
end
```

Code Listing 3: The Uninitialized function.

APPENDIX B: MATLAB SCRIPT FOR DATA ANALYSIS

```

close all; clear all; clc;
addpath('C:\Users\user\Desktop\university\final year project
jl\EEGLab\eeGLab new\extract file\eeGLab2021.1');
eeglab;
close all;

%% Read EEGData
EEG_raw=pop_loadset('C:\Users\user\Desktop\OpenVibe\EEG data
collection\SUB 6\Section 6\S6_Sess6_EC_3min_Raw.set');
EEG_clean=pop_loadset('C:\Users\user\Desktop\OpenVibe\EEG data
collection\SUB 6\Section 6\S6_Sess6_EC_3min_Clean.set');
data_raw = EEG_raw.data;
data_clean = EEG_clean.data;

%% for 10 min data
y = 10*128*60/2;
x=length(data_clean)/2;
data_clean = data_clean(:,x-y:x+y-1);
x=length(data_raw)/2;
data_raw = data_raw(:,x-y:x+y-1);

%% Calculate RMSE and Correlation
RMSE = mean(mean(sqrt((1/length(data_raw))*(data_raw(:,:)-
data_clean(:,:)).^2)));
corr = corr2(data_raw,data_clean);

%% End

```

Code Listing 4: The MATLAB script for calculating the correlation and RMSE.

```

close all; clear all; clc;
addpath('C:\Users\userR\Desktop\university\final_year_project
j1\EEGLab\eeGLab new\extract file\eeGLab2021.1\');
path1 = 'C:\Users\userR\Desktop\OpenVibe\EEG data collection\SUB
6\Section 6\';
addpath(path);
addpath('C:\Users\userR\Desktop\OpenVibe\Power');
path = strcat(path1, '*.set');
list = dir(fullfile(path));

% eeGLab
delta = [0.5 4];
theta = [4 8];
alpha = [8 13];
beta = [13 30];
gamma = [30 40];
deltapow = [];
thetapow = [];
alphapow = [];
betapow = [];
gammapow = [];
for i = 1:length(list)
    EEG = pop_loadset(strcat(list(i).folder, '\', list(i).name));
    data = EEG.data;

    temp = split(list(i).name, '_');
    sess = str2double(string(temp(3)));
    temp2 = split(string(temp(1)), 'S');
    sub = str2double(string(temp2(2)));

    winsize = 1*EEG.srate; % 2-sec window
    hannw = .5 - cos(2*pi*linspace(0,1,winsize))./2;
    Overlap = round(winsize*(75/100)); % overlap in percentage
    nfft = EEG.srate*4;

    for chani = 1:EEG.nbchan
        [pxx, freq] =
pwelch(squeeze(data(chani, :, :)), hannw, Overlap, nfft, EEG.srate);
        powarray(:, chani) = mean(pxx, 2);

        %define the indices for each EEG band
        deltaIdx = dsearchn(freq, delta');
        thetaIdx = dsearchn(freq, theta');
        alphaIdx = dsearchn(freq, alpha');
        betaIdx = dsearchn(freq, beta');
        gammaIdx = dsearchn(freq, gamma');
    end

    BLdeltapow =
mean( powarray(deltaIdx(1):deltaIdx(2), :, :) ,1); %take the mean at
first dimension to get one value for each channel
    BLthetapow = mean( powarray(thetaIdx(1):thetaIdx(2), :, :) ,1);
    BLalphapow = mean( powarray(alphaIdx(1):alphaIdx(2), :, :) ,1);
    BLbetapow = mean( powarray(betaIdx(1):betaIdx(2), :, :) ,1);
    BLgammapow = mean( powarray(gammaIdx(1):gammaIdx(2), :, :) ,1);

```

```

%store the power of each EEG band separately
BLdeltapow = [sub, sess, BLdeltapow, mean(BLdeltapow)];
BLthetapow = [sub, sess, BLthetapow, mean(BLthetapow)];
BLalphapow = [sub, sess, BLalphapow, mean(BLalphapow)];
BLbetapow = [sub, sess, BLbetapow, mean(BLbetapow)];
BLgammapow = [sub, sess, BLgammapow, mean(BLgammapow)];
%clear the powarray variable for the next subject/session/file

deltapow = [deltapow; BLdeltapow];
thetapow = [thetapow; BLthetapow];
alphapow = [alphapow; BLalphapow];
betapow = [betapow ; BLbetapow];
gammapow = [gammapow; BLgammapow];

clear powarray;
end

deltaPowTable = table(deltapow);%,'VariableNames', {'Subject',
'Session', 'AF3', 'F7', 'F3', 'FC5', 'T7', 'P7', 'O1', 'O2', 'P8',
'T8', 'FC6', 'F4', 'F8', 'AF4', 'Mean'});
thetaPowTable = table(thetapow);%,'VariableNames', {'Subject',
'Session', 'AF3', 'F7', 'F3', 'FC5', 'T7', 'P7', 'O1', 'O2', 'P8',
'T8', 'FC6', 'F4', 'F8', 'AF4', 'Mean'});
alphaPowTable = table(alphapow);%,'VariableNames', {'Subject',
'Session', 'AF3', 'F7', 'F3', 'FC5', 'T7', 'P7', 'O1', 'O2', 'P8',
'T8', 'FC6', 'F4', 'F8', 'AF4', 'Mean'});
betaPowTable = table(betapow);%,'VariableNames', {'Subject',
'Session', 'AF3', 'F7', 'F3', 'FC5', 'T7', 'P7', 'O1', 'O2', 'P8',
'T8', 'FC6', 'F4', 'F8', 'AF4', 'Mean'});
gammaPowTable = table(gammapow);%,'VariableNames', {'Subject',
'Session', 'AF3', 'F7', 'F3', 'FC5', 'T7', 'P7', 'O1', 'O2', 'P8',
'T8', 'FC6', 'F4', 'F8', 'AF4', 'Mean'});

% addpath('C:\Users\Danyal Mahmood\Desktop\');
FName =
'C:\Users\userR\Desktop\OpenVibe\Power\PowerAnalysis_S6_Section6.xlsx
';
writetable(deltaPowTable, FName, 'Sheet', 'Delta')
writetable(thetaPowTable, FName, 'Sheet', 'Theta');
writetable(alphaPowTable, FName, 'Sheet', 'Alpha');
writetable(betaPowTable , FName, 'Sheet', 'Beta');
writetable(gammaPowTable, FName, 'Sheet', 'Gamma');

```

Code Listing 5: The MATLAB script for calculating the Alpha power.